


# Theory of superconducting qubits beyond the lumped-element approximation

Ari Mizel<sup>✉\*</sup>

Laboratory for Physical Sciences, 8050 Greenmead Drive, College Park, Maryland 20740, USA

 (Received 5 April 2023; revised 4 December 2023; accepted 19 January 2024; published 15 February 2024)

In the design and investigation of superconducting qubits and related devices, a lumped-element circuit model is the standard theoretical approach. However, many important physical questions lie beyond its scope, such as the behavior of circuits with strong Josephson junctions carrying substantial currents and the properties of very small superconducting devices. By performing gauge transformations on self-consistent solutions of the Bogoliubov–de Gennes equations, we develop here a formalism that treats Josephson couplings nonperturbatively. We apply the formalism to (a) show that Fermi sea effects can contribute to the effective capacitance of small charge qubits; (b) demonstrate an asymmetry in clockwise and counterclockwise current states in small rf superconducting quantum interference device qubits; and (c) provide a microscopic wave function of superconducting Schrödinger cats suitable for computing the number of entangled electrons.

DOI: [10.1103/PhysRevApplied.21.024030](https://doi.org/10.1103/PhysRevApplied.21.024030)

## I. INTRODUCTION

Over the past quarter century, superconducting qubits [1] have attracted growing interest and excitement. Several remarkable families of superconducting qubits have been invented and investigated. Examples include charge, flux, phase, qutrit, transmon, and fluxonium qubits [2–8]. These families are distinguished from one another by circuit topology as well as circuit parameter values like capacitance and Josephson current [9]. Sustained study of superconducting qubits has yielded dramatic performance improvements. For instance, while coherence times of early qubits were of the order of nanoseconds [2], recent devices have achieved coherence times reaching milliseconds [10].

To describe these designer quantum systems, a quantum mechanical lumped-element (LE) circuit theory has been employed very broadly and successfully by researchers [11–13]. However, as the degree of control achieved over superconducting qubits becomes ever more exquisite [10, 14–23], a role is emerging for a theoretical description of increased detail and precision. In this paper, we frame such a description that, among its important features, treats the Josephson coupling between islands nonperturbatively.

As shown below, this theory can address physical questions that are beyond the scope of LE theory, such as the behavior of strong Josephson couplings supporting substantial currents or the properties of much smaller superconducting qubits. This description also has the potential to supply answers when ambiguities arise in the application of LE theory (for an example in the case of junctions

with Andreev bound states, see Ref. [24]) and to permit refined calculations of qubit properties such as perturbations of qubit spectroscopy. This paper presents sample calculations on a charge qubit (Sec. II) and on an rf superconducting quantum interference device (SQUID) qubit (Sec. III), showing consistency with LE theory and also revealing uncharted effects. In Sec. IV, we then leverage the microscopic character of our analysis to study the number of electrons in a superconducting “Schrödinger cat” [25–28]. We conclude in Sec. V.

## II. THEORY AND APPLICATION TO THE CHARGE QUBIT

LE theory describes a superconducting circuit as a system of distinct islands that are coupled weakly by Josephson junctions. The justification for this description typically involves treating a tunneling Hamiltonian at second order in perturbation theory [13,29,30]. To go beyond LE theory, and gain new insights, we holistically treat all of the coupled islands of the system as a single superconducting entity.

Assume a microscopic electronic Hamiltonian

$$H = T + P + W, \quad (1)$$

where the kinetic, potential, and interaction energies are

$$T = - \sum_{\mathbf{R}} \sum_{\mathbf{a}=\pm\mathbf{a}_x, \pm\mathbf{a}_y, \pm\mathbf{a}_z} c_{\mathbf{r}+\mathbf{a},\sigma}^\dagger t_{\mathbf{r}+\mathbf{a},\mathbf{r}} c_{\mathbf{r},\sigma}, \quad (2)$$

\*ari@arimizel.com

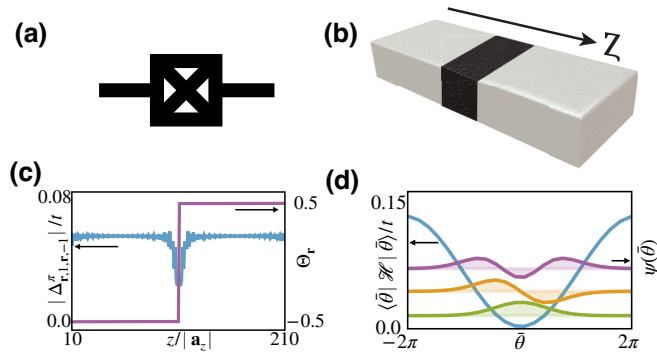


FIG. 1. (a) Circuit diagram of a charge qubit. (b) Schematic of a qubit with a Josephson junction in the dark region. Results of the simulation described in the text appear in (c) and (d). (c) Magnitude (blue) of the superconducting gap  $|\Delta_{\mathbf{r},\sigma=1,\mathbf{r},\sigma'=-1}^r|$  depends on the  $z$  component of  $\mathbf{r}$ . Minimum at the Josephson junction is evident. Rescaled phase function  $\Theta_r$  (purple). (d) Diagonal elements  $\langle\theta|\mathcal{H}|\theta\rangle$ , corresponding to Josephson energy (blue). Energy eigenstates of Eq. (12) shown in green, orange, and purple.

$$P = \sum_{\mathbf{R}} (v(\mathbf{r}) - \mu) c_{\mathbf{R}}^\dagger c_{\mathbf{R}}, \quad (3)$$

$$W = \frac{1}{2} \sum_{\mathbf{R},\mathbf{R}'} W(\mathbf{R},\mathbf{R}') c_{\mathbf{R}}^\dagger c_{\mathbf{R}'}^\dagger c_{\mathbf{R}'} c_{\mathbf{R}}. \quad (4)$$

Here,  $\mathbf{R} \equiv (\mathbf{r}, \sigma)$  is a combined position and spin coordinate introduced for notational brevity. The operator  $c_{\mathbf{R}} = c_{\mathbf{r},\sigma}$  destroys an electron with position  $\mathbf{r}$  and spin  $\sigma$ . The quantity  $t_{\mathbf{r}+\mathbf{a},\mathbf{r}}$  denotes a tunneling matrix element between site  $\mathbf{r}$  and site  $\mathbf{r} + \mathbf{a}$ . (Although the notation suggests a tight-binding approximation, this is inessential to our formalism: the sums over  $\mathbf{R}$  and  $\mathbf{a}$  in Eq. (2) could be replaced by an integral and  $t_{\mathbf{r}+\mathbf{a},\mathbf{r}}$  by the negative of a Laplacian operator.) In Eq. (3),  $v(\mathbf{r})$  gives the potential energy at  $\mathbf{r}$ , and  $\mu$  denotes the chemical potential of the system. The quantity  $W(\mathbf{R},\mathbf{R}')$  in Eq. (4) describes the interaction energy between electrons at  $\mathbf{R}$  and  $\mathbf{R}'$ .

Good descriptions of the low-energy eigenstates of  $H$  are obtained by following steps (i)–(iii) below. For concreteness, we focus on a charge qubit, or Cooper-pair box [2], comprising a superconducting grain with a junction region [Figs. 1(a) and 1(b)].

**Step (i)** of our approach defines a set of states that will be superposed to describe the low-energy eigenstates of Eq. (1). The choice of states is motivated by the following conventional rationale. Superconductors have low-energy excited states that allow them to conduct current. To develop intuition about the form of such current-carrying states, imagine boosting each electron in the ground state

by a momentum  $\hbar\delta\mathbf{q}$ . Such a boost multiplies the superconducting order parameter

$$\Delta_{\mathbf{R},\mathbf{R}'} = W(\mathbf{R},\mathbf{R}') \langle c_{\mathbf{R}} c_{\mathbf{R}'} \rangle \quad (5)$$

by a position-dependent phase  $e^{i\delta\mathbf{q}\cdot(\mathbf{r}+\mathbf{r}')}$ . This suggests that low-energy excitations can be expressed in terms of phase changes of the superconducting order parameter. Guided by this intuition, we define our set of states as follows.

For a charge qubit, the states are denoted  $|\theta\rangle$ , where  $\theta$  equals the phase drop of the superconducting order parameter from one end of the qubit to the other. The familiar LE approximation also works with a set of states  $|\theta\rangle$ . In our approach, however, we eschew the assumption of an abrupt phase drop at the Josephson junction and model the entire qubit holistically. One consequence is that our  $\theta$  is not restricted to  $(-\pi, \pi]$  as it is in the LE approximation: as the phase increments from one end of the qubit to the other, it can accumulate a large change of many multiples of  $2\pi$ .

We approximate the low-energy eigenstates of Eq. (1) by superposing many  $|\theta\rangle$ . One could imagine various mathematical definitions of the states  $|\theta\rangle$ , and it is not *a priori* evident which leads to the best results. Fortunately, one expects that predictions are somewhat insensitive to the precise form of the individual states  $|\theta\rangle$  since many  $|\theta\rangle$  will be superposed. In this paper, to obtain the state  $|\theta = 0\rangle$ , we self-consistently solve the Bogoliubov–de Gennes (BdG) equations [29,31], collecting the positive-energy eigenstates into matrices  $U_{\mathbf{R},\mathbf{K}}$  and  $V_{\mathbf{R},\mathbf{K}}$  (see Appendices A and B). Here,  $\mathbf{K} = (\mathbf{k}, \sigma)$  labels the solutions, with  $\mathbf{k}$  denoting some set of quantum numbers, but not necessarily the momentum.

To define  $|\theta\rangle$  for other values of  $\theta$ , one option is to repeat the BdG calculation, fixing the total phase change of the order parameter at  $\theta$ . To carry this out, one could return the order parameter phase, after each iteration toward self-consistency, to  $-\theta/2$  at one end of the qubit and  $\theta/2$  at the other end. Such a calculation produces an order parameter with a fixed total phase change, but whose local phase change depends upon  $\mathbf{r}$  according to the microscopic physics of Eq. (1): the phase changes rapidly where it is energetically advantageous to do so. In our case of a charge qubit, the phase will drop rapidly across the Josephson junction.

In this paper, we take a different approach to defining  $|\theta\rangle$  that reduces computational effort, leads to results that are more readily compared to the LE approximation, and is suitable for application to the rf SQUID as well as the charge qubit, as shown in Sec. III below. (In Appendix B, the two different approaches to computing  $|\theta\rangle$  are compared in the case  $\theta = \pi/2$  and are shown to produce similar states.) Instead of performing a self-consistent BdG calculation for all  $\theta$ , we do so for  $\theta = \pi$  and use the result to define  $|\theta\rangle$  for general  $\theta$  as follows. The calculation at

$\theta = \pi$  yields an order parameter  $\Delta_{\mathbf{R},\mathbf{R}'}$  with phase  $-\pi/2$  on one side of the system and  $\pi/2$  on the other. We rescale the phase of  $\Delta_{\mathbf{R},\mathbf{R}'}$ , defining

$$\Theta_{\mathbf{r}} = \text{Arg } \Delta_{(\mathbf{r},1),(\mathbf{r},-1)}^{\pi}, \quad (6)$$

which takes the value  $-1/2$  on one side of the system and  $1/2$  on the other. Then, we define  $|\theta\rangle$  as the state obtained by applying a gauge transformation to the  $\theta = 0$  self-consistent BdG solution

$$U_{\mathbf{R},\mathbf{K}} \rightarrow e^{i\theta\Theta_{\mathbf{r}}/2} U_{\mathbf{R},\mathbf{K}} \quad \text{and} \quad V_{\mathbf{R},\mathbf{K}} \rightarrow e^{-i\theta\Theta_{\mathbf{r}}/2} V_{\mathbf{R},\mathbf{K}}. \quad (7)$$

This ensures that the phase of the order parameter of  $|\theta\rangle$  indeed changes by  $\theta$  across the system. Having defined  $|\theta\rangle$ , we have completed step (i).

In **step (ii)** of our approach, each approximate low-energy eigenstate of  $H$  is written as a superposition of the states defined in step (i):  $|\psi\rangle = \sum_{\theta} \psi(\theta)|\theta\rangle$ .

Finally, **step (iii)** entails computing the wave function  $\psi(\theta)$  by solving the Schrödinger equation

$$\sum_{\theta} \langle \theta | H | \theta' \rangle \psi(\theta') = E \sum_{\theta} \langle \theta | \theta' \rangle \psi(\theta'). \quad (8)$$

The overlaps  $\langle \theta | \theta' \rangle$  appear on the right-hand side of this equation because the  $|\theta\rangle$  do not form an orthonormal basis in general. We can quantify  $\langle \theta | \theta' \rangle$  using the Onishi formula [32], a well-known result in the nuclear physics literature [33]. Given Eq. (7), the Onishi formula reduces to  $|\langle \theta | \theta' \rangle|^2 = \det \mathcal{U}$ , where

$$\mathcal{U}_{\mathbf{K},\mathbf{K}'} = \sum_{\mathbf{R}} U_{\mathbf{K},\mathbf{R}}^{\dagger} e^{-i(\theta-\theta')\Theta_{\mathbf{r}}/2} U_{\mathbf{R},\mathbf{K}'} + V_{\mathbf{K},\mathbf{R}}^{\dagger} e^{i(\theta-\theta')\Theta_{\mathbf{r}}/2} V_{\mathbf{R},\mathbf{K}'}. \quad (9)$$

By an appropriate choice of the phases of  $U_{\mathbf{R},\mathbf{K}}$  and  $V_{\mathbf{R},\mathbf{K}}$ , we ensure that  $\langle \theta | \theta' \rangle$  is real. Then,  $\langle \theta | \theta' \rangle = \pm \sqrt{\det \mathcal{U}}$ , with the sign determined by continuity starting from  $\langle \theta | \theta \rangle = 1$ .

The matrix elements  $\langle \theta | H | \theta' \rangle$  of Hamiltonian (1) can be computed using [33]

$$\frac{\langle \theta' | c_{\mathbf{R}_1}^{\dagger} c_{\mathbf{R}_2} | \theta \rangle}{\langle \theta' | \theta \rangle} = e^{i\theta\Theta_{\mathbf{r}_2}/2} \left( V^* \frac{1}{\mathcal{U}^T} V^T \right)_{\mathbf{R}_2, \mathbf{R}_1} e^{-i\theta'\Theta_{\mathbf{r}_1}/2} \quad (10)$$

and

$$\begin{aligned} \langle \theta' | c_{\mathbf{R}_1}^{\dagger} c_{\mathbf{R}_2}^{\dagger} c_{\mathbf{R}_3} c_{\mathbf{R}_4} | \theta \rangle / \langle \theta' | \theta \rangle &= e^{i\theta\Theta_{\mathbf{r}_4}/2} \left( V^* \frac{1}{\mathcal{U}^T} V^T \right)_{\mathbf{R}_4, \mathbf{R}_1} e^{-i\theta'\Theta_{\mathbf{r}_1}/2} e^{i\theta\Theta_{\mathbf{r}_3}/2} \left( V^* \frac{1}{\mathcal{U}^T} V^T \right)_{\mathbf{R}_3, \mathbf{R}_2} e^{-i\theta'\Theta_{\mathbf{r}_2}/2} \\ &\quad - e^{i\theta\Theta_{\mathbf{r}_3}/2} \left( V^* \frac{1}{\mathcal{U}^T} V^T \right)_{\mathbf{R}_3, \mathbf{R}_1} e^{-i\theta'\Theta_{\mathbf{r}_1}/2} e^{i\theta\Theta_{\mathbf{r}_4}/2} \left( V^* \frac{1}{\mathcal{U}^T} V^T \right)_{\mathbf{R}_4, \mathbf{R}_2} e^{-i\theta'\Theta_{\mathbf{r}_2}/2} \\ &\quad - e^{-i\theta\Theta_{\mathbf{r}_1}/2} \left( U^* \frac{1}{\mathcal{U}^T} U^T \right)_{\mathbf{R}_1, \mathbf{R}_2} e^{-i\theta'\Theta_{\mathbf{r}_2}/2} e^{i\theta\Theta_{\mathbf{r}_4}/2} \left( V^* \frac{1}{\mathcal{U}^T} U^T \right)_{\mathbf{R}_4, \mathbf{R}_3} e^{i\theta'\Theta_{\mathbf{r}_3}/2}. \end{aligned} \quad (11)$$

The Onishi formula and the matrix elements (10) and (11) are derived in Appendix C. Having computed these quantities, we solve Eq. (8). Various technical details of the calculation are described in Appendices D and E. It is convenient to find the solution by orthonormalizing the basis  $|\theta\rangle$ . We denote the state vectors of the orthonormalized basis using an overbar, as in  $|\bar{\theta}\rangle$ , and the effective Hamiltonian in this basis as  $\mathcal{H}$ . Equation (8) then takes the form

$$\sum_{\bar{\theta}} \langle \bar{\theta} | \mathcal{H} | \bar{\theta}' \rangle \bar{\psi}(\bar{\theta}') = E \bar{\psi}(\bar{\theta}). \quad (12)$$

This formalism is suitable for first-principles or phenomenological computation as well as analytical study. Here we present an example computation, carrying out steps (i)–(iii) on a model charge qubit formed by a rectangular lattice of  $5 \times 5 \times 220$  tight-binding sites with  $a =$

$|\mathbf{a}_x| = |\mathbf{a}_y| = |\mathbf{a}_z|$ . The tunneling matrix element in Eq. (2) between adjacent lattice sites is set to an energy  $t$ , except we set  $t_{\mathbf{r}+\mathbf{a}_z, \mathbf{r}} = 0.1t$  across a single plane in the center of the system to form the Josephson junction. In Eq. (3), the potential is set to  $v(\mathbf{r}) = 0$ , and the chemical potential is set to  $\mu = -3.42t$ , leading to a mean occupation of 1012 electrons in the system. We follow standard practice in BdG computations by modeling the electron-electron attraction that produces superconductivity using a Hubbard interaction [29–31]. In particular, in Eq. (4), we choose a spin-independent interaction of the form

$$W(\mathbf{r}, \sigma; \mathbf{r}', \sigma') = \begin{cases} -g, & \mathbf{r} = \mathbf{r}', \\ \lambda, & \mathbf{r} \neq \mathbf{r}', \\ |\mathbf{r} - \mathbf{r}'|, & \end{cases} \quad (13)$$

Computations show that  $g = 2.25t$  gives rise to a superconducting gap of reasonable magnitude [Fig. 1(c)] despite

the nearly one-dimensional geometry of the system. The Coulomb repulsion is incorporated into the formalism, but it is taken negligibly small to avoid disrupting the electron-electron attraction that produces superconductivity ( $\lambda = 5 \times 10^{-5}ta$ ). These choices of  $g$  and  $\lambda$  lead to a qubit in the BdG simulation with a tractable number of tight-binding sites that has reasonable superconducting properties; future explorations of parameter space are envisioned.

The results are best described by making reference to the Hamiltonian of a charge qubit in the LE approximation

$$H_{LE} = 4E_C n^2 + E_J(1 - \cos \bar{\theta}). \quad (14)$$

In this equation,  $\bar{\theta}$  is an operator corresponding to the phase drop across the Josephson junction, and  $n$  is the excess number of Cooper pairs on one island of the qubit; these operators satisfy the commutation relation  $[\bar{\theta}, n] = i$ . The parameter  $E_C = e^2/2C$  is defined in terms of the mutual capacitance  $C$  of the two islands of the qubit and the electron charge  $e$ . The Josephson coupling  $E_J$  characterizes the strength of tunneling across the junction.

The diagonal matrix elements of our effective Hamiltonian,  $\langle \bar{\theta} | \mathcal{H} | \bar{\theta} \rangle$ , correspond to the Josephson term in Eq. (14) and originate from terms in Eq. (2) associated with hopping across the junction. They are plotted in Fig. 1(d). The off-diagonal elements of  $\langle \bar{\theta} | \mathcal{H} | \bar{\theta}' \rangle$  cause transitions from one value of  $|\bar{\theta}\rangle$  to another; they correspond to the capacitive term in Eq. (14). Based on LE theory, one expects this term to arise from Eq. (4). However, in our calculations Eq. (4) makes only a small contribution that even deviates from the quadratic  $4E_C n^2$  form; presumably this is because the Coulomb interaction in Eq. (13) is negligible compared to the short-ranged Hubbard interaction for our choice of parameters. Surprisingly, the kinetic energy (2) makes the dominant contribution. The physical reason is that transferring  $n$  Cooper pairs across our small charge qubit shrinks the Fermi sea of one half of the superconducting grain and grows the Fermi sea of the other. Expanding the total energy of the two Fermi seas in  $n$  gives a quadratic term  $(8E_F/3N_{\text{tot}})n^2$ , where  $E_F$  and  $N_{\text{tot}}$  respectively denote the Fermi energy and number of electrons on each island of the charge qubit (see Appendix F).

It may be possible to amplify and exploit such underexplored capacitance features in device designs. While the contribution  $(8E_F/3N_{\text{tot}})n^2$  is negligible for large qubits such as transmons, it is potentially relevant for smaller devices. (We estimate the dimensions of a capacitor island of a transmon [34,35] as  $250 \mu\text{m} \times 500 \mu\text{m} \times 50 \text{nm}$ . Using the density  $\rho_{\text{Al}} = 2.7 \text{g/cm}^3$  and  $E_F = 11 \text{eV}$  of Al, one finds that  $8E_F/3N_{\text{tot}} \sim 10^{-7} \text{GHz}$ . For a merged-element transmon island [36] of area  $A = 1 \mu\text{m}^2$  and thickness  $50 \text{nm}$ , without an antenna,  $8E_F/3N_{\text{tot}} \sim 10^{-2} \text{GHz}$ . These values should be compared to a typical transmon capacitive energy of order  $1 \text{GHz}$ .)

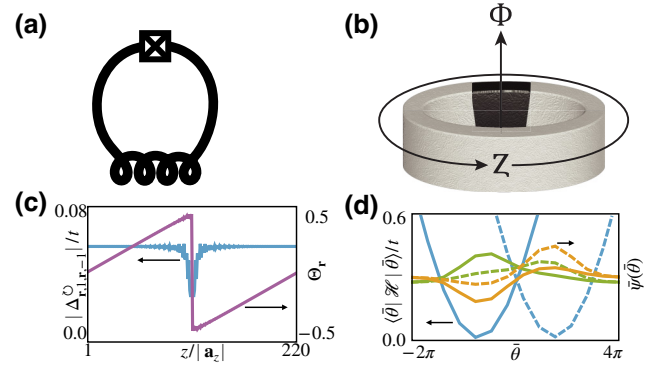


FIG. 2. (a) Circuit diagram of an rf-SQUID qubit. (b) Schematic of a qubit; magnetic flux  $\Phi = h/4e$  threads the loop. Results of the simulation described in the text appear in (c) and (d). (c) Magnitude (blue) of the superconducting gap  $|\Delta_{\mathbf{r},\sigma=1,\mathbf{r},\sigma'=-1}^{\odot}|$  depends only on the  $z$  component of  $\mathbf{r}$ . Rescaled phase function  $\Theta_r$  (purple). (d) Diagonal elements  $\langle \odot, \bar{\theta} | \mathcal{H} | \odot, \bar{\theta} \rangle$  (solid) and  $\langle \odot, \theta | \mathcal{H} | \odot, \bar{\theta} \rangle$  (dashed) form the effective potential (the shorthand notation  $\langle \bar{\theta} | \mathcal{H} | \bar{\theta} \rangle$  on the  $y$  axis implies both  $\langle \odot, \bar{\theta} | \mathcal{H} | \odot, \bar{\theta} \rangle$  and  $\langle \odot, \theta | \mathcal{H} | \odot, \bar{\theta} \rangle$ ). Ground state (green) and first excited state (yellow) each has a counterclockwise (solid) and clockwise (dashed) component [the shorthand notation  $\psi(\bar{\theta})$  on the  $y$  axis implies both  $\psi(\odot, \bar{\theta})$  and  $\psi(\odot, \theta)$ ].

The eigenstates in Fig. 1(d) take a form in consonance with the LE solution of Eq. (14). Indeed, Eq. (14) arises from our formalism in the appropriate abrupt-junction limit, as shown in Appendix F.

### III. APPLICATION TO THE rf-SQUID QUBIT

We now turn from a charge qubit to a more complicated example: an rf-SQUID qubit threaded by magnetic flux [see Figs. 2(a) and 2(b)]. In this case, step (i) involves more than one type of self-consistent BdG solution:  $|\odot, \theta^{\odot}\rangle$  carries a current circulating clockwise around the loop and  $|\odot, \theta^{\ominus}\rangle$  carries a current circulating counterclockwise. (If the Josephson energy of the junction is sufficiently large compared to the inductive energy of the loop, still more self-consistent solutions arise; they are easily included in the analysis if needed.) The corresponding self-consistent BdG solutions are collected into matrices  $U_{\mathbf{R},\mathbf{K}}^{\odot}$ ,  $V_{\mathbf{R},\mathbf{K}}^{\odot}$  and  $U_{\mathbf{R},\mathbf{K}}^{\ominus}$ ,  $V_{\mathbf{R},\mathbf{K}}^{\ominus}$ , respectively. The associated order parameters are  $\Delta_{\mathbf{R},\mathbf{R}'}^{\odot}$  and  $\Delta_{\mathbf{R},\mathbf{R}'}^{\ominus}$ . The phase drop  $\theta^{\odot}$  equals the change in  $\text{Arg} \Delta_{(\mathbf{r},1),(\mathbf{r},-1)}^{\odot}$  along the inductance of the loop (i.e., the total phase change of the order parameter around the loop minus the phase change across the junction). This is computed as the difference between the maximum and minimum values of  $\text{Arg} \Delta_{(\mathbf{r},1),(\mathbf{r},-1)}^{\odot}$ . The phase drop  $\theta^{\ominus}$  is defined analogously.

Next, we define states  $|\odot, \theta\rangle$  and  $|\ominus, \theta\rangle$  for a general phase drop  $\theta$ . As in the charge qubit case, one could imagine performing a self-consistent BdG calculation, fixing the phase drop along the inductance of the loop after



each iteration toward self-consistency. (Although such an approach is complicated by the fact that, because of the loop geometry of the qubit, there are no self-evident positions at which to fix phases.) However, again as for the charge qubit, we take a different approach. We define a rescaled phase function in analogy to Eq. (6). In this case, we set

$$\Theta_{\mathbf{r}} = \text{Arg } \Delta_{(\mathbf{r},1),(\mathbf{r},-1)}^{\circ} / \theta^{\circ}. \quad (15)$$

Note that Eq. (15) is defined using  $\Delta_{\mathbf{R},\mathbf{R}'}^{\circ}$  rather than  $\Delta_{\mathbf{R},\mathbf{R}'}^{\circ}$ ; this choice is made so  $\Theta_{\mathbf{r}}$  does not have any vortices that accumulate multiples of  $2\pi$  as  $\Theta_{\mathbf{r}}$  proceeds around the qubit loop. This property is evident in Fig. 2(c). If the direction of applied flux were flipped,  $\Delta_{\mathbf{R},\mathbf{R}'}^{\circ}$  would appear in the definition instead.

In terms of Eq. (15),  $|\circ, \theta\rangle$  is defined as the BdG state obtained by performing a gauge transformation  $U_{\mathbf{R},\mathbf{K}}^{\circ} \rightarrow e^{i(\theta-\theta^{\circ})\Theta_{\mathbf{r}}/2} U_{\mathbf{R},\mathbf{K}}^{\circ}$  and  $V_{\mathbf{R},\mathbf{K}}^{\circ} \rightarrow e^{-i(\theta-\theta^{\circ})\Theta_{\mathbf{r}}/2} V_{\mathbf{R},\mathbf{K}}^{\circ}$ . This definition ensures that the phase of the order parameter of  $|\circ, \theta\rangle$  changes by  $\theta$  instead of  $\theta^{\circ}$  along the inductor. Analogously,  $|\ominus, \theta\rangle$  is defined as the BdG state obtained by performing a gauge transformation  $U_{\mathbf{R},\mathbf{K}}^{\circ} \rightarrow e^{i(\theta-\theta^{\circ})\Theta_{\mathbf{r}}/2} U_{\mathbf{R},\mathbf{K}}^{\circ}$  and  $V_{\mathbf{R},\mathbf{K}}^{\circ} \rightarrow e^{-i(\theta-\theta^{\circ})\Theta_{\mathbf{r}}/2} V_{\mathbf{R},\mathbf{K}}^{\circ}$ .

In step (ii), we write

$$|\psi\rangle = \sum_{\theta} \psi(\circ, \theta) |\circ, \theta\rangle + \psi(\ominus, \theta) |\ominus, \theta\rangle. \quad (16)$$

Step (iii) then requires us to solve

$$\begin{aligned} & \sum_{\theta'} \begin{bmatrix} \langle \circ, \theta | H | \circ, \theta' \rangle & \langle \circ, \theta | H | \ominus, \theta' \rangle \\ \langle \ominus, \theta | H | \circ, \theta' \rangle & \langle \ominus, \theta | H | \ominus, \theta' \rangle \end{bmatrix} \begin{bmatrix} \psi(\circ, \theta') \\ \psi(\ominus, \theta') \end{bmatrix} \\ & = E \sum_{\theta'} \begin{bmatrix} \langle \circ, \theta | \circ, \theta' \rangle & \langle \circ, \theta | \ominus, \theta' \rangle \\ \langle \ominus, \theta | \circ, \theta' \rangle & \langle \ominus, \theta | \ominus, \theta' \rangle \end{bmatrix} \begin{bmatrix} \psi(\circ, \theta') \\ \psi(\ominus, \theta') \end{bmatrix}. \end{aligned} \quad (17)$$

After transforming to an orthonormal basis with states  $|\bar{\circ}, \bar{\theta}\rangle$ ,  $|\bar{\ominus}, \bar{\theta}\rangle$  denoted using an overbar, we produce a  $2 \times 2$  effective Hamiltonian  $\mathcal{H}$ .

We carry out steps (i)–(iii), performing a numerical computation on a model rf-SQUID qubit analogous to the charge qubit computation above. The  $5 \times 5 \times 220$  lattice is retained, but, to capture the loop geometry, periodic boundary conditions are imposed in the  $z$  direction. To incorporate the magnetic flux  $h/4e$  threading the loop, tunneling matrix elements in the  $z$  direction are assigned a phase according to  $t_{\mathbf{r}+\mathbf{a}_z, \mathbf{r}} = te^{-i\pi/2(220)}$ , while  $t_{\mathbf{r}+\mathbf{a}_z, \mathbf{r}} = 0.3te^{-i\pi/2(220)}$  at the junction. Other tunneling matrix elements are set to  $t$ . Because of the  $2 \times 2$  structure of matrix  $\mathcal{H}$ , its diagonal gives rise to the two potentials  $\langle \bar{\circ}, \bar{\theta} | \mathcal{H} | \bar{\circ}, \bar{\theta} \rangle$  and  $\langle \bar{\ominus}, \bar{\theta} | \mathcal{H} | \bar{\ominus}, \bar{\theta} \rangle$  depicted in Fig. 2(d); the curve formed by taking the lower potential at each  $\bar{\theta}$

produces an rf-SQUID double-well potential as expected. Indeed, under suitable conditions discussed in Appendix F,  $\mathcal{H}$  reduces to the LE Hamiltonian

$$H_{\text{LE}} = 4E_C n^2 + E_J(1 - \cos \bar{\theta}) + E_L(\bar{\theta} - \phi)^2/2, \quad (18)$$

where  $\bar{\theta} \in \mathbb{R}$  is unbounded,  $[\bar{\theta}, n] = i$ , and  $\phi = 2\pi(2e/h)\Phi$  is fixed by the applied flux  $\Phi$ .

The energy eigenstates of  $\mathcal{H}$ , shown in Fig. 2(d), accord with those expected within LE theory. However, they exhibit an asymmetry between the two peaks of each wave function, best seen by comparing the solid and dashed green lines in Fig. 2(d). This asymmetry arises for the following reason. The microscopic electronic Hamiltonian (1) possesses an exact symmetry at half an electronic flux quantum  $h/2e$ , but not at half a superconducting flux quantum  $h/4e$ . At  $h/4e$ , the symmetry between clockwise and counterclockwise superconducting states in the loop emerges only approximately when electrons bind into Cooper pairs of charge  $2e$ . Since this binding is incomplete in mesoscopic scale qubits [37]—qubits with length scales under the superconducting coherence length—the wave function exhibits asymmetry. This effect is captured by our formalism, but neglected in LE theory in which complete binding of electrons in Cooper pairs is taken for granted. The effect might be observable in Al superconducting qubits with dimensions smaller than  $1 \mu\text{m}$ , the scale of the superconducting coherence length.

#### IV. SCHRÖDINGER CAT STATES

The microscopic character of our theory makes it particularly suitable for investigating Schrödinger cat states in superconducting loops. Several remarkable experiments [25,26] have realized these cats, formed by superposing a clockwise supercurrent and a counterclockwise supercurrent. To assess the implications [38] of these experiments, it is of central importance to quantify the size of the cat—the number of entangled particles. We focus on Ref. [25] since it raises the breathtaking possibility that billions of electrons might have been entangled.

Computing the number of entangled electrons,  $\Delta N$ , is beyond the scope of LE theory, as discussed in Appendix G. The state-of-the-art calculation is due to Korsbakken *et al.* [27,28]. Given a partition of the many-body Schrödinger cat state into two terms  $\sqrt{1/2} |\circ\rangle + \sqrt{1/2} |\ominus\rangle$ , they introduced

$$\Delta N = \frac{1}{2} \sum_{\mathbf{Q}} |\langle \circ | c_{\mathbf{Q}}^{\dagger} c_{\mathbf{Q}} | \circ \rangle - \langle \ominus | c_{\mathbf{Q}}^{\dagger} c_{\mathbf{Q}} | \ominus \rangle| \quad (19)$$

to count how many particles are in different modes in  $|\circ\rangle$  and  $|\ominus\rangle$ . Here,  $\mathbf{Q}$  labels a state in whichever basis of single-particle electron states maximizes  $\Delta N$ , which is the basis in which the matrix  $\langle \circ | c_{\mathbf{Q}}^{\dagger} c_{\mathbf{Q}} | \circ \rangle - \langle \ominus | c_{\mathbf{Q}}^{\dagger} c_{\mathbf{Q}} | \ominus \rangle$

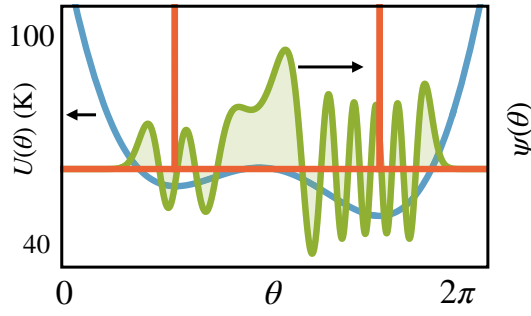


FIG. 3. LE theory potential  $E_J(1 - \cos\theta) + \frac{1}{2}E_L(\theta - \phi)^2$  is shown in blue. LE wave function of the Schrödinger cat state of Ref. [25] is shown in green. The two-symmetric-peak form assumed by Korsbakken *et al.* [27,28] is depicted in red. We use parameters that are suitable for Ref. [25]:  $E_C = 9.0$  mK = 0.19 GHz,  $E_J = 76$  K = 1.6 THz,  $E_L = 645$  K = 13.5 THz, and  $\phi = 2\pi(0.51425)$ .

is diagonal. Korsbakken *et al.* evaluated Eq. (19) by approximating  $|\odot\rangle$  and  $|\ominus\rangle$  as Galilean-boosted BCS states rather than using LE theory. They thereby derived the approximation  $\Delta N = 3IL_z/4ev_F$ . A compact derivation of this result appears in Appendix G. As a check, we evaluate Eq. (19) using the rf-SQUID qubit eigenstates that we obtained numerically above. For these, their approximation differs from Eq. (19) by about 30%.

Applying their approximation to the experiment [25], they concluded [27,28] that  $\Delta N \sim 3800\text{--}5750$  electrons. However, note that the wave function realized experimentally in Ref. [25] takes the form of the green curve in Fig. 3 according to LE theory. It differs dramatically from a Schrödinger cat form  $\sqrt{1/2}|\odot\rangle + \sqrt{1/2}|\ominus\rangle$  and particularly so from the pristine wave function assumed by Korsbakken *et al.* [27,28] (red curve in Fig. 3). A definitive evaluation of the number of entangled electrons in Ref. [25] would therefore require a tractable alternative to Eq. (19) that does not assume a Schrödinger cat form  $\sqrt{1/2}|\odot\rangle + \sqrt{1/2}|\ominus\rangle$ . Unfortunately, defining such a metric is a vexatious problem [39] out of the scope of our study.

## V. CONCLUSION

In conclusion, we have developed a microscopic theory of superconducting qubits that goes beyond the standard LE approximation. It accords with LE theory both for charge and rf-SQUID qubits and yields several insights inaccessible to LE theory. Numerous applications of this tool are anticipated as experimental progress allows increasingly precise study of superconducting qubits. For instance, it would be particularly interesting to incorporate microscopic calculations of qubit decoherence by adding impurities or other sources of environmental noise in Eq. (1).

## ACKNOWLEDGMENTS

We gratefully thank M. Kruger and I. M. Mandelberg for key suggestions.

## APPENDIX A: BOGOLIUBOV–DE GENNES EQUATIONS

In this appendix we derive the BdG equations, following Ref. [29, pp. 137–145]. We begin with the definition of the Bogoliubov transformation

$$\begin{aligned} c_{\mathbf{R}} &= \sum_{\mathbf{K}} U_{\mathbf{R},\mathbf{K}} \alpha_{\mathbf{K}} + V_{\mathbf{R},\mathbf{K}}^* \alpha_{\mathbf{K}}^\dagger, \\ c_{\mathbf{R}}^\dagger &= \sum_{\mathbf{K}} U_{\mathbf{R},\mathbf{K}}^* \alpha_{\mathbf{K}}^\dagger + V_{\mathbf{R},\mathbf{K}} \alpha_{\mathbf{K}}. \end{aligned} \quad (\text{A1})$$

Imposing anticommutation relations, we obtain

$$\{c_{\mathbf{R}}, c_{\mathbf{R}'}\} = V_{\mathbf{R},\mathbf{K}}^* U_{\mathbf{R}',\mathbf{K}} + U_{\mathbf{R},\mathbf{K}} V_{\mathbf{R}',\mathbf{K}}^* = 0, \quad (\text{A2})$$

which becomes

$$V^* U^T + U V^\dagger = 0 \quad (\text{A3})$$

as a matrix equation. Similarly,

$$\{c_{\mathbf{R}}, c_{\mathbf{R}'}^\dagger\} = U_{\mathbf{R},\mathbf{K}} U_{\mathbf{R}',\mathbf{K}}^* + V_{\mathbf{R},\mathbf{K}}^* V_{\mathbf{R}',\mathbf{K}} = \delta_{\mathbf{R},\mathbf{R}'}, \quad (\text{A4})$$

where a Kronecker delta appears on the right-hand side. As a matrix equation, this becomes

$$U U^\dagger + V^* V^T = I. \quad (\text{A5})$$

Now, the Bogoliubov transformation (A1) can be written as a matrix equation

$$\begin{bmatrix} c_{\mathbf{R}} \\ c_{\mathbf{R}}^\dagger \end{bmatrix} = \begin{bmatrix} U & V^* \\ V & U^* \end{bmatrix} \begin{bmatrix} \alpha_{\mathbf{R}} \\ \alpha_{\mathbf{R}}^\dagger \end{bmatrix}. \quad (\text{A6})$$

Relations (A3) and (A5) imply that

$$\begin{bmatrix} U & V^* \\ V & U^* \end{bmatrix} \begin{bmatrix} U^\dagger & V^\dagger \\ V^T & U^T \end{bmatrix} = \begin{bmatrix} I & 0 \\ 0 & I \end{bmatrix}. \quad (\text{A7})$$

Since the right inverse of a square matrix is also a left inverse, we also have

$$\begin{bmatrix} U^\dagger & V^\dagger \\ V^T & U^T \end{bmatrix} \begin{bmatrix} U & V^* \\ V & U^* \end{bmatrix} = \begin{bmatrix} I & 0 \\ 0 & I \end{bmatrix}. \quad (\text{A8})$$

This equation gives two identities; collecting them together with Eqs. (A3) and (A5) gives a total of four identities:

$$\begin{aligned} U U^\dagger + V^* V^T &= I, & U^\dagger U + V^\dagger V &= I, \\ V^* U^T + U V^\dagger &= 0, & V^T U + U^T V &= 0. \end{aligned} \quad (\text{A9})$$

Equation (A8) implies that the inverse of the Bogoliubov transformation is

$$\begin{aligned}\alpha_{\mathbf{K}} &= \sum_{\mathbf{R}} U_{\mathbf{R},\mathbf{K}}^* c_{\mathbf{R}} + V_{\mathbf{R},\mathbf{K}}^* c_{\mathbf{R}}^\dagger, \\ \alpha_{\mathbf{K}}^\dagger &= \sum_{\mathbf{R}} U_{\mathbf{R},\mathbf{K}} c_{\mathbf{R}}^\dagger + V_{\mathbf{R},\mathbf{K}} c_{\mathbf{R}}.\end{aligned}\quad (\text{A10})$$

We use the Bogoliubov transformation to find eigenstates of a mean-field approximation to the Hamiltonian. Starting with

$$H = \sum_{\mathbf{R},\mathbf{R}'} c_{\mathbf{R}}^\dagger h_{\mathbf{R}',\mathbf{R}} c_{\mathbf{R}} + \frac{1}{2} W(\mathbf{R}', \mathbf{R}) c_{\mathbf{R}}^\dagger c_{\mathbf{R}}^\dagger c_{\mathbf{R}} c_{\mathbf{R}'}, \quad (\text{A11})$$

we make a mean-field approximation

$$\begin{aligned}H' &= \sum_{\mathbf{R},\mathbf{R}'} c_{\mathbf{R}}^\dagger h_{\mathbf{R}',\mathbf{R}} c_{\mathbf{R}} + \frac{1}{2} W(\mathbf{R}', \mathbf{R}) [c_{\mathbf{R}'}^\dagger c_{\mathbf{R}'} \langle c_{\mathbf{R}}^\dagger c_{\mathbf{R}} \rangle + \langle c_{\mathbf{R}'}^\dagger c_{\mathbf{R}'} \rangle c_{\mathbf{R}}^\dagger c_{\mathbf{R}} - \langle c_{\mathbf{R}'}^\dagger c_{\mathbf{R}'} \rangle \langle c_{\mathbf{R}}^\dagger c_{\mathbf{R}} \rangle \\ &\quad - c_{\mathbf{R}'}^\dagger c_{\mathbf{R}} \langle c_{\mathbf{R}}^\dagger c_{\mathbf{R}'} \rangle - \langle c_{\mathbf{R}'}^\dagger c_{\mathbf{R}} \rangle c_{\mathbf{R}}^\dagger c_{\mathbf{R}'} + \langle c_{\mathbf{R}'}^\dagger c_{\mathbf{R}} \rangle \langle c_{\mathbf{R}}^\dagger c_{\mathbf{R}'} \rangle \\ &\quad + c_{\mathbf{R}}^\dagger c_{\mathbf{R}}^\dagger \langle c_{\mathbf{R}} c_{\mathbf{R}'} \rangle + \langle c_{\mathbf{R}}^\dagger c_{\mathbf{R}}^\dagger \rangle c_{\mathbf{R}} c_{\mathbf{R}'} - \langle c_{\mathbf{R}}^\dagger c_{\mathbf{R}}^\dagger \rangle \langle c_{\mathbf{R}} c_{\mathbf{R}'} \rangle].\end{aligned}\quad (\text{A12})$$

In each of the three lines in brackets, we have paired the first operator  $c_{\mathbf{R}'}^\dagger$  in the interaction term  $\frac{1}{2} W(\mathbf{R}', \mathbf{R}) c_{\mathbf{R}}^\dagger c_{\mathbf{R}}^\dagger c_{\mathbf{R}} c_{\mathbf{R}'}$  with one of the remaining three operators ( $c_{\mathbf{R}'}^\dagger$  is paired with  $c_{\mathbf{R}'}^\dagger$  in the first line, then  $c_{\mathbf{R}}$  in the second line, then  $c_{\mathbf{R}}^\dagger$  in the third line). Within each line, we applied the approximation

$$\begin{aligned}ab &= [(a - \langle a \rangle) + \langle a \rangle][\langle b \rangle + (b - \langle b \rangle)] \\ &\approx (a - \langle a \rangle)\langle b \rangle + \langle a \rangle(b - \langle b \rangle) + \langle a \rangle\langle b \rangle \\ &= a\langle b \rangle + \langle a \rangle b - \langle a \rangle\langle b \rangle,\end{aligned}$$

taking  $a$  to be the product of  $c_{\mathbf{R}'}^\dagger$  and its pair, and taking  $b$  to be the product of the remaining two operators. The approximation assumes that  $(a - \langle a \rangle)(b - \langle b \rangle)$  is the product of two small quantities and can be neglected. It is convenient to set

$$\begin{aligned}H' &\equiv \sum_{\mathbf{R},\mathbf{R}'} c_{\mathbf{R}}^\dagger h'_{\mathbf{R}',\mathbf{R}} c_{\mathbf{R}} + \frac{\Delta_{\mathbf{R}',\mathbf{R}}}{2} c_{\mathbf{R}}^\dagger c_{\mathbf{R}}^\dagger + \frac{(\Delta_{\mathbf{R}',\mathbf{R}})^*}{2} c_{\mathbf{R}} c_{\mathbf{R}'} \\ &\quad + \text{const},\end{aligned}\quad (\text{A13})$$

where

$$\Delta_{\mathbf{R}',\mathbf{R}} = W(\mathbf{R}, \mathbf{R}') \langle c_{\mathbf{R}} c_{\mathbf{R}'} \rangle \quad (\text{A14})$$

and

$$\begin{aligned}h'_{\mathbf{R}',\mathbf{R}} &= h_{\mathbf{R}',\mathbf{R}} + \delta_{\mathbf{R}',\mathbf{R}} \sum_{\mathbf{R}''} W(\mathbf{R}, \mathbf{R}'') \langle c_{\mathbf{R}''}^\dagger c_{\mathbf{R}''} \rangle \\ &\quad - W(\mathbf{R}, \mathbf{R}') \langle c_{\mathbf{R}}^\dagger c_{\mathbf{R}'} \rangle.\end{aligned}\quad (\text{A15})$$

To obtain this form of  $h'_{\mathbf{R}',\mathbf{R}}$ , we have used  $W(\mathbf{R}, \mathbf{R}') = W(\mathbf{R}', \mathbf{R})$ . Note that the final term of  $h'_{\mathbf{R}',\mathbf{R}}$  is the exchange interaction.

We next demand that the Bogoliubov transformation diagonalize the mean-field Hamiltonian, so that  $H' = E_g + \sum_{\mathbf{K}} \epsilon_{\mathbf{K}} \alpha_{\mathbf{K}}^\dagger \alpha_{\mathbf{K}}$ . This implies that  $[\alpha_{\mathbf{K}}, H'] = \epsilon_{\mathbf{K}} \alpha_{\mathbf{K}}$  and  $[\alpha_{\mathbf{K}}^\dagger, H'] = -\epsilon_{\mathbf{K}} \alpha_{\mathbf{K}}^\dagger$ . We compute

$$[c_{\mathbf{R}}, H'] = \sum_{\mathbf{R}'} h'_{\mathbf{R},\mathbf{R}'} c_{\mathbf{R}'} + \Delta_{\mathbf{R},\mathbf{R}'} c_{\mathbf{R}'}^\dagger \quad (\text{A16})$$

and substitute in the Bogoliubov transformation (A1). Comparing the coefficients of  $\alpha_{\mathbf{K}}$  and  $\alpha_{\mathbf{K}}^\dagger$  on each side, we obtain the two BdG equations

$$\begin{aligned}\epsilon_{\mathbf{K}} U_{\mathbf{R},\mathbf{K}} &= \sum_{\mathbf{R}'} h'_{\mathbf{R},\mathbf{R}'} U_{\mathbf{R}',\mathbf{K}} + \Delta_{\mathbf{R},\mathbf{R}'} V_{\mathbf{R}',\mathbf{K}}, \\ \epsilon_{\mathbf{K}} V_{\mathbf{R},\mathbf{K}} &= \sum_{\mathbf{R}'} (-h'_{\mathbf{R},\mathbf{R}'})^* V_{\mathbf{R}',\mathbf{K}} + (\Delta_{\mathbf{R},\mathbf{R}'})^* U_{\mathbf{R}',\mathbf{K}}.\end{aligned}\quad (\text{A17})$$

Substituting the Bogoliubov transformations into the definitions of  $h'_{\mathbf{R}',\mathbf{R}}$  and  $\Delta_{\mathbf{R}',\mathbf{R}}$  and using the fact that  $\alpha_{\mathbf{K}}$  annihilates the ground state, we obtain

$$\begin{aligned}h'_{\mathbf{R}',\mathbf{R}} &= h_{\mathbf{R}',\mathbf{R}} + \delta_{\mathbf{R}',\mathbf{R}} \sum_{\mathbf{R}''} W(\mathbf{R}, \mathbf{R}'') \sum_{\mathbf{K}} V_{\mathbf{R}'',\mathbf{K}} V_{\mathbf{R}'',\mathbf{K}}^* \\ &\quad - W(\mathbf{R}, \mathbf{R}') \sum_{\mathbf{K}} V_{\mathbf{R},\mathbf{K}} V_{\mathbf{R}',\mathbf{K}}^*\end{aligned}\quad (\text{A18})$$

and

$$\Delta_{\mathbf{R}',\mathbf{R}} = W(\mathbf{R}, \mathbf{R}') \sum_{\mathbf{K}} U_{\mathbf{R},\mathbf{K}} V_{\mathbf{R}',\mathbf{K}}^* \quad (\text{A19})$$

The BdG equations are to be solved self-consistently with these expressions for  $h'_{\mathbf{R}',\mathbf{R}}$  and  $\Delta_{\mathbf{R}',\mathbf{R}}$ .

It is sometimes useful to express the BdG many-body ground state in Thouless form [33]. To do so, we define  $Z \equiv (VU^{-1})^*$  and write

$$|0\rangle = \mathcal{N} \exp \left[ \frac{1}{2} \sum_{\mathbf{R}, \mathbf{R}'} c_{\mathbf{R}}^\dagger Z_{\mathbf{R}, \mathbf{R}'} c_{\mathbf{R}'}^\dagger \right] |\text{vac}\rangle. \quad (\text{A20})$$

Here,  $\mathcal{N}$  is a normalization constant. This is a generalization of the standard BCS ground-state wave function  $\mathcal{N} \exp[\sum_{\mathbf{k}} (v_{\mathbf{k}}/u_{\mathbf{k}}) c_{\mathbf{k},1}^\dagger c_{-\mathbf{k},-1}^\dagger] |\text{vac}\rangle$ . It is more general because it does not assume the Cooper pairs form specifically in the momentum basis.

To show that Eq. (A20) is the many-body ground state of the BdG equations, we need to demonstrate that it is annihilated by  $\alpha_{\mathbf{K}}$ . Using the inverse Bogoliubov transformation (A10), we compute

$$\left[ \frac{1}{2} \sum_{\mathbf{R}, \mathbf{R}'} c_{\mathbf{R}}^\dagger Z_{\mathbf{R}, \mathbf{R}'} c_{\mathbf{R}'}^\dagger, \alpha_{\mathbf{K}} \right] = \sum_{\mathbf{R}} V_{\mathbf{R}, \mathbf{K}}^* c_{\mathbf{R}}^\dagger. \quad (\text{A21})$$

The argument uses identities (A9). Note that the right-hand side commutes with  $\frac{1}{2} \sum_{\mathbf{R}, \mathbf{R}'} c_{\mathbf{R}}^\dagger Z_{\mathbf{R}, \mathbf{R}'} c_{\mathbf{R}'}^\dagger$ . Now, according to a well-known lemma,

$$e^X Y e^{-X} = Y + [Y, X] \quad (\text{A22})$$

when  $[X, [X, Y]] = 0$ . (This is proven straightforwardly by differentiating  $e^{sX} Y e^{-sX}$  with respect to  $s$ .) Thus, we deduce that

$$\begin{aligned} & \exp \left[ -\frac{1}{2} \sum_{\mathbf{R}, \mathbf{R}'} c_{\mathbf{R}}^\dagger Z_{\mathbf{R}, \mathbf{R}'} c_{\mathbf{R}'}^\dagger \right] \alpha_{\mathbf{K}} \exp \left[ \frac{1}{2} \sum_{\mathbf{R}, \mathbf{R}'} c_{\mathbf{R}}^\dagger Z_{\mathbf{R}, \mathbf{R}'} c_{\mathbf{R}'}^\dagger \right] \\ &= \alpha_{\mathbf{K}} - \sum_{\mathbf{R}} V_{\mathbf{R}, \mathbf{K}}^* c_{\mathbf{R}}^\dagger \\ &= \sum_{\mathbf{R}} U_{\mathbf{R}, \mathbf{K}}^* c_{\mathbf{R}}. \end{aligned} \quad (\text{A23})$$

It follows that

$$\begin{aligned} & \alpha_{\mathbf{K}} \exp \left[ \frac{1}{2} \sum_{\mathbf{R}, \mathbf{R}'} c_{\mathbf{R}}^\dagger Z_{\mathbf{R}, \mathbf{R}'} c_{\mathbf{R}'}^\dagger \right] |\text{vac}\rangle = \exp \left[ \frac{1}{2} \sum_{\mathbf{R}, \mathbf{R}'} c_{\mathbf{R}}^\dagger Z_{\mathbf{R}, \mathbf{R}'} c_{\mathbf{R}'}^\dagger \right] \\ & \times \sum_{\mathbf{R}} U_{\mathbf{R}, \mathbf{K}}^* c_{\mathbf{R}} |\text{vac}\rangle = 0. \end{aligned} \quad (\text{A24})$$

We see that Eq. (A20) is indeed the many-body ground state of the BdG equations.

The states  $|\theta\rangle$  are defined in the text using the gauge transformation  $U_{\mathbf{R}, \mathbf{K}} \rightarrow e^{i\theta \Theta_{\mathbf{r}}/2} U_{\mathbf{R}, \mathbf{K}}$  and  $V_{\mathbf{R}, \mathbf{K}} \rightarrow e^{-i\theta \Theta_{\mathbf{r}}/2} V_{\mathbf{R}, \mathbf{K}}$ . Given the form (A20) for  $|0\rangle$ , this implies that

$$|\theta\rangle = \mathcal{N} \exp \left[ \frac{1}{2} \sum_{\mathbf{R}, \mathbf{R}'} e^{i\theta(\Theta_{\mathbf{r}} + \Theta_{\mathbf{r}'})/2} c_{\mathbf{R}}^\dagger Z_{\mathbf{R}, \mathbf{R}'} c_{\mathbf{R}'}^\dagger \right] |\text{vac}\rangle. \quad (\text{A25})$$

## APPENDIX B: COMPUTATIONAL SOLUTION OF THE BOGOLIUBOV–DE GENNES EQUATIONS

Our formalism is compatible with detailed first-principles approaches to solving the BdG equations. However, in this paper, for simplicity, we model the superconducting qubits using a rectangular lattice with lattice vectors  $\mathbf{a}_x$ ,  $\mathbf{a}_y$ , and  $\mathbf{a}_z$ . The number of tight-binding sites in the  $x$ ,  $y$ , and  $z$  directions are  $N_x$ ,  $N_y$ , and  $N_z$ , respectively, giving rise to lengths  $L_x = N_x |\mathbf{a}_x|$ ,  $L_y = N_y |\mathbf{a}_y|$ , and  $L_z = N_z |\mathbf{a}_z|$ . Symmetries can facilitate solution of the BdG equations. We employ periodic boundary conditions in the  $x$  and  $y$  directions; as a result of the translational symmetry, our self-consistent quantities (A18) and (A19) are homogeneous in the  $x$  and  $y$  directions.

We choose a spin-independent interaction of the form

$$\begin{aligned} W(\mathbf{r}, \sigma; \mathbf{r}', \sigma') &= w(x - x', y - y', z - z') \\ &= \begin{cases} -g, & \mathbf{r} = \mathbf{r}', \\ \lambda, & \mathbf{r} \neq \mathbf{r}', \end{cases} \end{aligned} \quad (\text{B1})$$

where the attractive Hubbard interaction at  $\mathbf{r} = \mathbf{r}'$  gives rise to superconductivity. The BdG equations can be written as

$$\begin{aligned} \epsilon_k U_{m_x, m_y, z, \sigma, \mathbf{K}} &= \sum_{z', \sigma'} h'_{m_x, m_y, z, \sigma, z', \sigma'} U_{m_x, m_y, z', \sigma', \mathbf{K}} \\ &+ \Delta_{m_x, m_y, z, \sigma, z', \sigma'} V_{m_x, m_y, z', \sigma', \mathbf{K}}, \end{aligned} \quad (\text{B2a})$$

$$\begin{aligned} \epsilon_k V_{m_x, m_y, z, \sigma, \mathbf{K}} &= \sum_{z', \sigma'} (-h'_{-m_x, -m_y, z, \sigma, z', \sigma'})^* V_{m_x, m_y, z', \sigma', \mathbf{K}} \\ &+ (\Delta_{-m_x, -m_y, z, \sigma, z', \sigma'})^* U_{m_x, m_y, z', \sigma', \mathbf{K}}, \end{aligned} \quad (\text{B2b})$$

where the transverse momenta  $2\pi m_x/L_x$  and  $2\pi m_y/L_y$  are good quantum numbers and

$$\begin{aligned} U_{m_x, m_y, z, \sigma, \mathbf{K}} &= \frac{1}{\sqrt{N_x N_y}} \sum_{x, y} e^{-i2\pi m_x x/L_x - i2\pi m_y y/L_y} U_{x, y, z, \sigma, \mathbf{K}}, \\ V_{m_x, m_y, z, \sigma, \mathbf{K}} &= \frac{1}{\sqrt{N_x N_y}} \sum_{x, y} e^{-i2\pi m_x x/L_x - i2\pi m_y y/L_y} V_{x, y, z, \sigma, \mathbf{K}}, \end{aligned} \quad (\text{B3})$$

with inverse relations

$$\begin{aligned} U_{x, y, z, \sigma, \mathbf{K}} &= \frac{1}{\sqrt{N_x N_y}} \sum_{m_x, m_y} e^{i2\pi m_x x/L_x + i2\pi m_y y/L_y} U_{m_x, m_y, z, \sigma, \mathbf{K}}, \\ V_{x, y, z, \sigma, \mathbf{K}} &= \frac{1}{\sqrt{N_x N_y}} \sum_{m_x, m_y} e^{i2\pi m_x x/L_x + i2\pi m_y y/L_y} V_{m_x, m_y, z, \sigma, \mathbf{K}}. \end{aligned} \quad (\text{B4})$$



To specify the forms of the operators on the right-hand side of Eqs. (B2), we define

$$\begin{aligned} & \frac{1}{N_x N_y} \sum_{x,y,x',y'} e^{-i2\pi \ell_x x/L_x - i2\pi \ell_y y/L_y} e^{i2\pi m_x x'/L_x - i2\pi m_y y'/L_y} h_{x,y,z,\sigma,x',y',z,\sigma'} \\ & \equiv \delta_{\ell_x, m_x} \delta_{\ell_y, m_y} h_{m_x, m_y, z, \sigma, z', \sigma'}, \end{aligned} \quad (\text{B5})$$

where

$$h_{m_x, m_y, z, \sigma, z', \sigma'} = \sum_{x,y} e^{-i2\pi m_x (x-x')/L_x - i2\pi m_y (y-y')/L_y} h_{x,y,z,\sigma,x',y',z,\sigma'}. \quad (\text{B6})$$

This definition is reasonable because  $h_{x,y,z,\sigma,x',y',z,\sigma'}$  depends on  $x$ ,  $x'$ ,  $y$ , and  $y'$  only via  $x - x'$  and  $y - y'$ . (The use of periodic boundary conditions in the  $x$  and  $y$  directions is essential for this translational invariance.) Similarly, we define

$$\begin{aligned} & \frac{1}{N_x N_y} \sum_{x,y,x',y'} e^{-i2\pi \ell_x x/L_x - i2\pi \ell_y y/L_y} e^{i2\pi m_x x'/L_x - i2\pi m_y y'/L_y} w(x - x', y - y', z - z') \\ & \equiv \delta_{\ell_x, m_x} \delta_{\ell_y, m_y} \tilde{w}(m_x, m_y, z - z'). \end{aligned} \quad (\text{B7})$$

Here, we have

$$\begin{aligned} \tilde{w}(m_x, m_y, z - z') &= \sum_{x,y} e^{-i2\pi m_x (x-x')/L_x - i2\pi m_y (y-y')/L_y} w(x - x', y - y', z - z') \\ &= N_x N_y s(m_x, m_y) e^{-2\pi \sqrt{(m_x/L_x)^2 + (m_y/L_y)^2} |z-z'|} - \sum_{n_x, n_y} s(n_x, n_y) \delta_{z, z'} - g \delta_{z, z'} \end{aligned} \quad (\text{B8})$$

with

$$s(m_x, m_y) = \frac{\lambda}{L_x L_y} \begin{cases} 2\sqrt{\pi L_x L_y}, & m_x = m_y = 0, \\ 1, & \text{otherwise.} \end{cases} \quad (\text{B9})$$

Then,

$$\begin{aligned} h'_{m_x, m_y, z', \sigma', z, \sigma} &= h_{m_x, m_y, z', \sigma', z, \sigma} \\ &+ \delta_{z', z} \delta_{\sigma', \sigma} \sum_{z'', \sigma''} \tilde{w}(0, 0, z - z'') \frac{1}{N_x N_y} \sum_{\ell_x, \ell_y, \mathbf{K}} V_{\ell_x, \ell_y, z'', \sigma'', \mathbf{K}} V_{\ell_x, \ell_y, z'', \sigma'', \mathbf{K}}^* \\ &- \sum_{\ell_x, \ell_y} \tilde{w}(m_x - \ell_x, m_y - \ell_y, z - z') \frac{1}{N_x N_y} \sum_{\mathbf{K}} V_{\ell_x, \ell_y, z, \sigma, \mathbf{K}} V_{\ell_x, \ell_y, z', \sigma', \mathbf{K}}^* \end{aligned} \quad (\text{B10})$$

and

$$\Delta_{m_x, m_y, z, \sigma, z', \sigma'} = \sum_{\ell_x, \ell_y} \tilde{w}(m_x + \ell_x, m_y + \ell_y, z - z') \frac{1}{N_x N_y} \sum_{\mathbf{K}} U_{\ell_x, \ell_y, z', \sigma', \mathbf{K}} V_{\ell_x, \ell_y, z, \sigma, \mathbf{K}}^*. \quad (\text{B11})$$

Alternatively, we also have

$$\Delta_{m_x, m_y, z, \sigma, z', \sigma'} = - \sum_{\ell_x, \ell_y} \tilde{w}(m_x - \ell_x, m_y - \ell_y, z - z') \frac{1}{N_x N_y} \sum_{\mathbf{K}} U_{\ell_x, \ell_y, z, \sigma, \mathbf{K}} V_{\ell_x, \ell_y, z', \sigma', \mathbf{K}}^* \quad (\text{B12})$$

The total energy of the system is given by

$$\begin{aligned} \langle H \rangle = & \sum_{\ell_x, \ell_y, z, \sigma, z', \sigma'} [h_{\ell_x, \ell_y, z, \sigma, z', \sigma'} \rho_{\ell_x, \ell_y, z, \sigma, z', \sigma'} + \frac{1}{2N_x N_y} \sum_{m_x, m_y} \tilde{w}(0, 0, z - z') \rho_{\ell_x, \ell_y, z, \sigma, z, \sigma} \rho_{m_x, m_y, z', \sigma', z', \sigma'} \\ & - \tilde{w}(\ell_x - m_x, \ell_y - m_y, z - z') \rho_{\ell_x, \ell_y, z', \sigma', z, \sigma} \rho_{m_x, m_y, z, \sigma, z', \sigma'} + \tilde{w}(\ell_x - m_x, \ell_y - m_y, z - z') \kappa_{\ell_x, \ell_y, z, \sigma, z', \sigma'}^* \kappa_{m_x, m_y, z, \sigma, z', \sigma'}]. \end{aligned} \quad (\text{B13})$$

Here,

$$\rho_{x, y, z, \sigma, x', y', z', \sigma'} = \langle c_{\mathbf{R}'}^\dagger c_{\mathbf{R}} \rangle = \sum_{\mathbf{K}} V_{x', y', z', \sigma', \mathbf{K}} V_{x, y, z, \sigma, \mathbf{K}}^* \quad (\text{B14})$$

leading to

$$\begin{aligned} \rho_{\ell_x, \ell_y, z, \sigma, z', \sigma'} &= \sum_{x, y} e^{-i2\pi \ell_x (x - x') / L_x - i2\pi \ell_y (y - y') / L_y} \rho_{x, y, z, \sigma, x', y', z', \sigma'} \\ &= \sum_{\mathbf{K}} V_{-\ell_x, -\ell_y, z', \sigma', \mathbf{K}} V_{-\ell_x, -\ell_y, z, \sigma, \mathbf{K}}^* \end{aligned} \quad (\text{B15})$$

with the minus signs in front of  $\ell_x$  and  $\ell_y$  in the final expression resulting from the flip in the order of the primed and unprimed variables in Eq. (B14). Similarly,

$$\kappa_{x, y, z, \sigma, x', y', z', \sigma'} = \langle c_{\mathbf{R}'} c_{\mathbf{R}} \rangle = \sum_{\mathbf{K}} U_{x', y', z', \sigma', \mathbf{K}} V_{x, y, z, \sigma, \mathbf{K}}^* \quad (\text{B16})$$

and

$$\begin{aligned} \kappa_{\ell_x, \ell_y, z, \sigma, z', \sigma'} &= \sum_{x, y} e^{-i2\pi \ell_x (x - x') / L_x - i2\pi \ell_y (y - y') / L_y} \kappa_{x, y, z, \sigma, x', y', z', \sigma'} \\ &= \sum_{\mathbf{K}} U_{-\ell_x, -\ell_y, z', \sigma', \mathbf{K}} V_{-\ell_x, -\ell_y, z, \sigma, \mathbf{K}}^*. \end{aligned} \quad (\text{B17})$$

In the main text, we describe numerical simulations for a charge qubit and for an rf-SQUID qubit performed using this framework. In the charge qubit case, the self-consistent solution to the BdG equations is labeled  $|\theta = 0\rangle$ . The main text describes the computation of additional states  $|\theta\rangle$  using a modified self-consistent procedure that fixes a given phase drop  $\theta$  by returning the order parameter phase, after each iteration toward self-consistency, to  $-\theta/2$  at one end of the qubit and  $\theta/2$  at the other end. Carrying out this procedure for  $\theta = \pi$  and again for  $\theta = \pi/2$  yields states  $|\theta = \pi\rangle_{\text{BdG}}$  and  $|\theta = \pi/2\rangle_{\text{BdG}}$ . The subscript BdG emphasizes that these states were obtained by self-consistent solution of the BdG equations. As described in the main text, the  $\theta = \pi$  solution is used to define  $|\theta\rangle$  via Eq. (7). In particular, we can define  $|\theta = \pi/2\rangle$  this way. It is then of interest to compare  $|\theta = \pi/2\rangle$  to  $|\theta = \pi/2\rangle_{\text{BdG}}$ . We find that the magnitude of the order parameters of the two states agree everywhere to within 3%. The phases of the order parameters of the two states differ near the Josephson junction, as shown in Fig. 4.

### APPENDIX C: DERIVATION OF THE MATRIX ELEMENTS

As described in the text, we need to compute the matrix elements that appear in the Schrödinger equations (8) and (17). For concreteness, we focus on the charge qubit case (8); the rf-SQUID case is very similar. The desired matrix elements take the form  $\langle \theta'' | \mathcal{O} | \theta' \rangle = \langle \theta'' | \mathcal{O} (c_{\mathbf{R}_1}^\dagger, c_{\mathbf{R}_2}) | \theta' \rangle$ , where the right-hand side makes explicit the dependence of  $\mathcal{O}$  on the operators  $c_{\mathbf{R}_1}^\dagger$  and  $c_{\mathbf{R}_2}$ . To compute these matrix elements, we follow the derivation in Ref. [33].

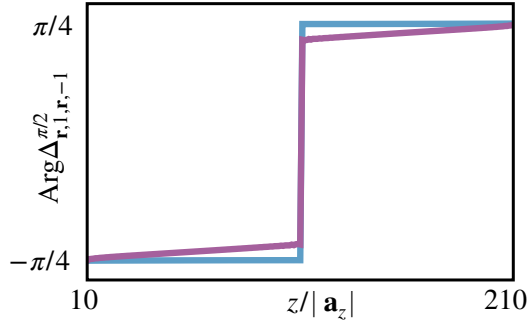


FIG. 4. Comparison of phases of the order parameters of the two states  $|\theta = \pi/2\rangle_{\text{BdG}}$  (purple) and  $|\theta = \pi/2\rangle$  (blue). Close overall agreement is evident, with the phase of the order parameter of  $|\theta = \pi/2\rangle$  changing slightly more abruptly near the Josephson junction.

The states  $|\theta'\rangle$  and  $|\theta''\rangle$  are defined in the text by performing gauge transformations from the BdG solutions of Eqs. (A17):

$$\begin{aligned} U'_{\mathbf{R},\mathbf{K}} &= e^{i\theta'\Theta_r/2} U_{\mathbf{R},\mathbf{K}}, & V'_{\mathbf{R},\mathbf{K}} &= e^{-i\theta'\Theta_r/2} V_{\mathbf{R},\mathbf{K}}, \\ U''_{\mathbf{R},\mathbf{K}} &= e^{i\theta''\Theta_r/2} U_{\mathbf{R},\mathbf{K}}, & V''_{\mathbf{R},\mathbf{K}} &= e^{-i\theta''\Theta_r/2} V_{\mathbf{R},\mathbf{K}}. \end{aligned} \quad (\text{C1})$$

These equations imply that  $|\theta'\rangle$  is annihilated by the quasiparticle operator  $\beta_{\mathbf{K}}$ , where

$$\begin{aligned} c_{\mathbf{R}} &= \sum_{\mathbf{L}} U'_{\mathbf{R},\mathbf{L}} \beta_{\mathbf{L}} + (V')_{\mathbf{R},\mathbf{L}}^* \beta_{\mathbf{L}}^\dagger, \\ c_{\mathbf{R}}^\dagger &= \sum_{\mathbf{L}} (U')_{\mathbf{R},\mathbf{L}}^* \beta_{\mathbf{L}}^\dagger + V'_{\mathbf{R},\mathbf{L}} \beta_{\mathbf{L}}, \end{aligned} \quad (\text{C2})$$

and  $|\theta''\rangle$  is annihilated by the quasiparticle operator  $\gamma_{\mathbf{K}}$ , where

$$\begin{aligned} c_{\mathbf{R}} &= \sum_{\mathbf{L}} U''_{\mathbf{R},\mathbf{L}} \gamma_{\mathbf{L}} + (V'')_{\mathbf{R},\mathbf{L}}^* \gamma_{\mathbf{L}}^\dagger, \\ c_{\mathbf{R}}^\dagger &= \sum_{\mathbf{L}} (U'')_{\mathbf{R},\mathbf{L}}^* \gamma_{\mathbf{L}}^\dagger + V''_{\mathbf{R},\mathbf{L}} \gamma_{\mathbf{L}}. \end{aligned} \quad (\text{C3})$$

The inverses of these last definitions are

$$\begin{aligned} \gamma_{\mathbf{K}} &= \sum_{\mathbf{R}} (U'')_{\mathbf{R},\mathbf{K}}^* c_{\mathbf{R}} + (V'')_{\mathbf{R},\mathbf{K}}^* c_{\mathbf{R}}^\dagger, \\ \gamma_{\mathbf{K}}^\dagger &= \sum_{\mathbf{R}} U'_{\mathbf{R},\mathbf{K}} c_{\mathbf{R}}^\dagger + V'_{\mathbf{R},\mathbf{K}} c_{\mathbf{R}}; \end{aligned} \quad (\text{C4})$$

combined with Eqs. (C2), these imply that

$$\begin{aligned} \gamma_{\mathbf{K}} &= \sum_{\mathbf{L}} U_{\mathbf{L},\mathbf{K}}^* \beta_{\mathbf{L}} + \mathcal{V}_{\mathbf{L},\mathbf{K}}^* \beta_{\mathbf{L}}^\dagger, \\ \gamma_{\mathbf{K}}^\dagger &= \sum_{\mathbf{L}} U_{\mathbf{L},\mathbf{K}} \beta_{\mathbf{L}}^\dagger + \mathcal{V}_{\mathbf{L},\mathbf{K}} \beta_{\mathbf{L}}, \end{aligned} \quad (\text{C5})$$

where  $\mathcal{U} = (U')^\dagger U'' + (V')^\dagger V''$  and  $\mathcal{V} = (V'')^T U'' + (U')^T V''$ .

To proceed, we use Thouless's theorem, which asserts that Bogoliubov states  $|\theta''\rangle$  and  $|\theta'\rangle$  are related by

$$|\theta''\rangle = \langle \theta' | \theta'' \rangle e^{\sum_{\mathbf{K},\mathbf{K}'} \beta_{\mathbf{K}}^\dagger \mathcal{Z}_{\mathbf{K},\mathbf{K}'} \beta_{\mathbf{K}'}/2} |\theta'\rangle, \quad (\text{C6})$$

where  $\mathcal{Z} = (\mathcal{U}^{-1})^*$ . The theorem assumes that  $\langle \theta' | \theta'' \rangle \neq 0$ , which we will see implies that  $\mathcal{U}^{-1}$ , and therefore  $\mathcal{Z}$ , exists. To prove Thouless's theorem, one needs to show that  $\gamma_{\mathbf{K}}$  annihilates the expression on the right-hand side of Eq. (C6). The proof closely parallels the argument leading up to Eq. (A24) with  $\alpha_{\mathbf{K}}$ ,  $c_{\mathbf{R}}$ ,  $U_{\mathbf{R},\mathbf{K}}$ ,  $V_{\mathbf{R},\mathbf{K}}$ , and  $Z_{\mathbf{R},\mathbf{R}'}$  replaced by  $\gamma_{\mathbf{K}}$ ,  $\beta_{\mathbf{L}}$ ,  $U_{\mathbf{L},\mathbf{K}}$ ,  $V_{\mathbf{L},\mathbf{K}}$  and  $\mathcal{Z}_{\mathbf{K},\mathbf{K}'}$ , respectively. In the first step of the proof, we calculate

$$e^{\sum_{\mathbf{K},\mathbf{K}'} \beta_{\mathbf{K}'} \mathcal{Z}_{\mathbf{K},\mathbf{K}'}^* \beta_{\mathbf{K}}/2} \beta_{\mathbf{L}} e^{-\sum_{\mathbf{K},\mathbf{K}'} \beta_{\mathbf{K}'} \mathcal{Z}_{\mathbf{K},\mathbf{K}'}^* \beta_{\mathbf{K}}/2} = \beta_{\mathbf{L}} \quad (\text{C7})$$

and

$$\begin{aligned} & e^{\sum_{\mathbf{K},\mathbf{K}'} \beta_{\mathbf{K}'} \mathcal{Z}_{\mathbf{K},\mathbf{K}'}^* \beta_{\mathbf{K}}/2} \beta_{\mathbf{L}}^\dagger e^{-\sum_{\mathbf{K},\mathbf{K}'} \beta_{\mathbf{K}'} \mathcal{Z}_{\mathbf{K},\mathbf{K}'}^* \beta_{\mathbf{K}}/2} \\ &= \beta_{\mathbf{L}}^\dagger + \left[ \sum_{\mathbf{K},\mathbf{K}'} \beta_{\mathbf{K}'} \mathcal{Z}_{\mathbf{K},\mathbf{K}'}^* \beta_{\mathbf{K}}/2, \beta_{\mathbf{L}}^\dagger \right] \\ &= \beta_{\mathbf{L}}^\dagger - \sum_{\mathbf{K}'} \beta_{\mathbf{K}'} \mathcal{Z}_{\mathbf{K}',\mathbf{L}}^* \end{aligned} \quad (\text{C8})$$

by applying lemma (A22). Then, we employ definition (C4) to obtain the analogues of Eqs. (A23) and (A24). Note that Eq. (C6) reduces to Eq. (A20) when we set  $U'$  equal to the identity matrix and  $V'$  equal to the zero matrix.

Thouless's theorem allows us to evaluate the overlap  $\langle \theta' | \theta'' \rangle$ . To do this, we simplify our expression for  $|\theta''\rangle$  into a BCS-like form. The theorem of Bloch and Messiah states that there are unitary matrices  $C$  and  $D$  for which  $\bar{U} = D^\dagger U C^\dagger$  and  $\bar{V} = D^T V C^\dagger$  are real and take simple block-diagonal forms. The matrix  $\bar{U}$  has  $2 \times 2$  blocks of the form  $u_{\mathbf{J}} \begin{bmatrix} 1 & 0 \\ 0 & 1 \end{bmatrix}$  in which the two states  $\mathbf{J}$  and  $\bar{\mathbf{J}}$  are paired with  $u_{\mathbf{J}} = u_{\bar{\mathbf{J}}}$ . In the usual BCS case in which pairing occurs in the momentum basis, we would have  $\mathbf{J} = \mathbf{k}, \sigma$  and  $\bar{\mathbf{J}} = -\mathbf{k}, -\sigma$ . The matrix  $\bar{V}$  has  $2 \times 2$  blocks of the form  $v_{\mathbf{J}} \begin{bmatrix} 0 & 1 \\ -1 & 0 \end{bmatrix}$ , involving the same two states  $\mathbf{J}$  and  $\bar{\mathbf{J}}$ . The coefficients satisfy the normalization condition  $u_{\mathbf{J}}^2 + v_{\mathbf{J}}^2 = 1$ . Defining  $\hat{\beta}_{\mathbf{J}}^\dagger = \sum_{\mathbf{K}} \beta_{\mathbf{K}}^\dagger D_{\mathbf{K},\mathbf{J}}$  in terms of matrix  $D$ , we find that  $\sum_{\mathbf{K},\mathbf{K}'} \beta_{\mathbf{K}}^\dagger \mathcal{Z}_{\mathbf{K},\mathbf{K}'} \beta_{\mathbf{K}'}/2 = \sum_{\mathbf{J}} \hat{\beta}_{\mathbf{J}}^\dagger (v_{\mathbf{J}}/u_{\mathbf{J}}) \hat{\beta}_{\mathbf{J}}^\dagger$ . Thus,

$$\begin{aligned} |\theta''\rangle &= \langle \theta' | \theta'' \rangle \exp \left( \sum_{\mathbf{J}} \hat{\beta}_{\mathbf{J}}^\dagger \frac{v_{\mathbf{J}}}{u_{\mathbf{J}}} \hat{\beta}_{\mathbf{J}}^\dagger \right) |\theta'\rangle \\ &= \langle \theta' | \theta'' \rangle \Pi_{\mathbf{J}} \left( 1 + \hat{\beta}_{\mathbf{J}}^\dagger \frac{v_{\mathbf{J}}}{u_{\mathbf{J}}} \hat{\beta}_{\mathbf{J}}^\dagger \right) |\theta'\rangle \\ &= \langle \theta' | \theta'' \rangle \Pi_{\mathbf{J}} \frac{1}{u_{\mathbf{J}}} \Pi_{\mathbf{J}} \left( u_{\mathbf{J}} + \hat{\beta}_{\mathbf{J}}^\dagger v_{\mathbf{J}} \hat{\beta}_{\mathbf{J}}^\dagger \right) |\theta'\rangle. \end{aligned} \quad (\text{C9})$$

The normalization condition  $\langle \theta'' | \theta'' \rangle = 1$  then implies that  $|\langle \theta' | \theta'' \rangle|^2 = \Pi_{\mathbf{J}} u_{\mathbf{J}}^2 = \det \mathcal{U}$ . The Onishi formula

$|\langle \theta' | \theta'' \rangle|^2 = \det \mathcal{U}$  leaves the phase of  $\langle \theta' | \theta'' \rangle$  undetermined; by choosing the phases of  $U_{\mathbf{R},\mathbf{K}}$  and  $V_{\mathbf{R},\mathbf{K}}$  appropriately, we can ensure that  $\langle \theta' | \theta'' \rangle$  is real. Then, the correct

sign of  $\langle \theta' | \theta'' \rangle = \pm \sqrt{\det \mathcal{U}}$  is fixed using continuity in  $\theta''$  starting with  $\langle \theta' | \theta'' \rangle = 1$  at  $\theta'' = \theta'$ .

Using Thouless's theorem, we can also calculate matrix elements of the form

$$\begin{aligned} \langle \theta'' | \mathcal{O} | \theta' \rangle / \langle \theta'' | \theta' \rangle &= \langle \theta'' | \mathcal{O}(c_{\mathbf{R}_1}^\dagger, c_{\mathbf{R}_2}) | \theta' \rangle / \langle \theta'' | \theta' \rangle \\ &= \langle \theta' | e^{\sum_{\mathbf{K},\mathbf{K}'} \beta_{\mathbf{K}'} Z_{\mathbf{K},\mathbf{K}'}^* \beta_{\mathbf{K}}/2} \mathcal{O}(c_{\mathbf{R}_1}^\dagger, c_{\mathbf{R}_2}) | \theta' \rangle \\ &= \langle \theta' | e^{\sum_{\mathbf{K},\mathbf{K}'} \beta_{\mathbf{K}'} Z_{\mathbf{K},\mathbf{K}'}^* \beta_{\mathbf{K}}/2} \mathcal{O}(c_{\mathbf{R}_1}^\dagger, c_{\mathbf{R}_2}) e^{-\sum_{\mathbf{K},\mathbf{K}'} \beta_{\mathbf{K}'} Z_{\mathbf{K},\mathbf{K}'}^* \beta_{\mathbf{K}}/2} | \theta' \rangle \\ &= \langle \theta' | \mathcal{O}(e^{\sum_{\mathbf{K},\mathbf{K}'} \beta_{\mathbf{K}'} Z_{\mathbf{K},\mathbf{K}'}^* \beta_{\mathbf{K}}/2} c_{\mathbf{R}_1}^\dagger e^{-\sum_{\mathbf{K},\mathbf{K}'} \beta_{\mathbf{K}'} Z_{\mathbf{K},\mathbf{K}'}^* \beta_{\mathbf{K}}/2} \\ &\quad \times e^{\sum_{\mathbf{K},\mathbf{K}'} \beta_{\mathbf{K}'} Z_{\mathbf{K},\mathbf{K}'}^* \beta_{\mathbf{K}}/2} c_{\mathbf{R}_2} e^{-\sum_{\mathbf{K},\mathbf{K}'} \beta_{\mathbf{K}'} Z_{\mathbf{K},\mathbf{K}'}^* \beta_{\mathbf{K}}/2}) | \theta' \rangle, \end{aligned} \quad (\text{C10})$$

where we have inserted  $e^{\sum_{\mathbf{K},\mathbf{K}'} \beta_{\mathbf{K}'} Z_{\mathbf{K},\mathbf{K}'}^* \beta_{\mathbf{K}}/2} e^{-\sum_{\mathbf{K},\mathbf{K}'} \beta_{\mathbf{K}'} Z_{\mathbf{K},\mathbf{K}'}^* \beta_{\mathbf{K}}/2} = 1$  as needed between adjacent operators in  $\mathcal{O}$  to derive the final line.

To proceed, we insert Eqs. (C7) and (C8) into the definitions of the Bogoliubov operators (C2), obtaining

$$\begin{aligned} &e^{\sum_{\mathbf{K},\mathbf{K}'} \beta_{\mathbf{K}'} Z_{\mathbf{K},\mathbf{K}'}^* \beta_{\mathbf{K}}/2} c_{\mathbf{R}} e^{-\sum_{\mathbf{K},\mathbf{K}'} \beta_{\mathbf{K}'} Z_{\mathbf{K},\mathbf{K}'}^* \beta_{\mathbf{K}}/2} \\ &= \sum_{\mathbf{L}} U_{\mathbf{R},\mathbf{L}} \beta_{\mathbf{L}} + (V'_{\mathbf{R},\mathbf{L}})^* \left( \beta_{\mathbf{L}}^\dagger - \sum_{\mathbf{K}'} \beta_{\mathbf{K}'} Z_{\mathbf{K}',\mathbf{L}}^* \right) \end{aligned} \quad (\text{C11})$$

and

$$\begin{aligned} &e^{\sum_{\mathbf{K},\mathbf{K}'} \beta_{\mathbf{K}'} Z_{\mathbf{K},\mathbf{K}'}^* \beta_{\mathbf{K}}/2} c_{\mathbf{R}}^\dagger e^{-\sum_{\mathbf{K},\mathbf{K}'} \beta_{\mathbf{K}'} Z_{\mathbf{K},\mathbf{K}'}^* \beta_{\mathbf{K}}/2} \\ &= \sum_{\mathbf{L}} (U'_{\mathbf{R},\mathbf{L}})^* \left( \beta_{\mathbf{L}}^\dagger - \sum_{\mathbf{K}'} \beta_{\mathbf{K}'} Z_{\mathbf{K}',\mathbf{L}}^* \right) + V_{\mathbf{R},\mathbf{L}} \beta_{\mathbf{L}}. \end{aligned} \quad (\text{C12})$$

It follows that

$$\begin{aligned} \langle \theta'' | c_{\mathbf{R}_1}^\dagger c_{\mathbf{R}_2} | \theta' \rangle / \langle \theta'' | \theta' \rangle &= \sum_{\mathbf{L},\mathbf{L}'} (V'_{\mathbf{R}_1,\mathbf{L}} \delta_{\mathbf{L},\mathbf{L}'} - (U'_{\mathbf{R}_1,\mathbf{L}})^* Z_{\mathbf{L},\mathbf{L}'}^*) (V'_{\mathbf{R}_2,\mathbf{L}})^* \\ &= (V' (V')^\dagger - (U')^* \mathcal{Z}^\dagger (V')^\dagger)_{\mathbf{R}_1,\mathbf{R}_2} \\ &= \left( V' \mathcal{U} \frac{1}{\mathcal{U}} (V')^\dagger + (U')^* \mathcal{V} \frac{1}{\mathcal{U}} (V')^\dagger \right)_{\mathbf{R}_1,\mathbf{R}_2} \\ &= \left( V' ((U')^\dagger U'' + (V')^\dagger V'') \frac{1}{\mathcal{U}} (V')^\dagger + (U')^* ((V')^T U'' \right. \end{aligned}$$

$$\begin{aligned} &\left. + (U')^T V'' \right) \frac{1}{\mathcal{U}} (V')^\dagger \Big)_{\mathbf{R}_1,\mathbf{R}_2} \\ &= \left( (V')^* \frac{1}{\mathcal{U}^T} (V'')^T \right)_{\mathbf{R}_2,\mathbf{R}_1}. \end{aligned} \quad (\text{C13})$$

The third equality uses  $\mathcal{Z} = -\mathcal{Z}^T$ , and the final equality is derived using the orthogonality relations  $(U')^* (V')^T + V' (U')^\dagger = 0$  and  $(V')^* (V')^T + U' (U')^\dagger = I$ . Similarly,

$$\begin{aligned} \langle \theta'' | c_{\mathbf{R}_1}^\dagger c_{\mathbf{R}_2}^\dagger | \theta' \rangle / \langle \theta'' | \theta' \rangle &= -\langle \theta'' | c_{\mathbf{R}_2}^\dagger c_{\mathbf{R}_1}^\dagger | \theta' \rangle / \langle \theta'' | \theta' \rangle \\ &= -(V' (U')^\dagger - (U')^* \mathcal{Z}^\dagger (V')^\dagger)_{\mathbf{R}_2,\mathbf{R}_1} \\ &= -\left( (U')^* \frac{1}{\mathcal{U}^T} (V'')^T \right)_{\mathbf{R}_1,\mathbf{R}_2} \end{aligned} \quad (\text{C14})$$

and

$$\begin{aligned} \langle \theta'' | c_{\mathbf{R}_3} c_{\mathbf{R}_4} | \theta' \rangle / \langle \theta'' | \theta' \rangle &= (U' (V')^\dagger - (V')^* \mathcal{Z}^\dagger (V')^\dagger)_{\mathbf{R}_3,\mathbf{R}_4} \\ &= \left( (V')^* \frac{1}{\mathcal{U}^T} (U'')^T \right)_{\mathbf{R}_4,\mathbf{R}_3}. \end{aligned} \quad (\text{C15})$$

Finally, we have

$$\begin{aligned} \langle \theta'' | c_{\mathbf{R}_1}^\dagger c_{\mathbf{R}_2}^\dagger c_{\mathbf{R}_3} c_{\mathbf{R}_4} | \theta' \rangle / \langle \theta'' | \theta' \rangle &= (V' (V')^\dagger - (U')^* \mathcal{Z}^\dagger (V')^\dagger)_{\mathbf{R}_1,\mathbf{R}_4} (V' (V')^\dagger \\ &\quad - (U')^* \mathcal{Z}^\dagger (V')^\dagger)_{\mathbf{R}_2,\mathbf{R}_3} - (V' (V')^\dagger - (U')^* \mathcal{Z}^\dagger (V')^\dagger)_{\mathbf{R}_1,\mathbf{R}_3} \\ &\quad (V' (V')^\dagger - (U')^* \mathcal{Z}^\dagger (V')^\dagger)_{\mathbf{R}_2,\mathbf{R}_4} \\ &\quad + (V' (U')^\dagger - (U')^* \mathcal{Z}^\dagger (U')^\dagger)_{\mathbf{R}_1,\mathbf{R}_2}, \\ &\quad (U' (V')^\dagger - (V')^* \mathcal{Z}^\dagger (V')^\dagger)_{\mathbf{R}_3,\mathbf{R}_4} \end{aligned}$$

$$\begin{aligned}
&= \left( (V')^* \frac{1}{\mathcal{U}^T} (V'')^T \right)_{\mathbf{R}_4, \mathbf{R}_1} \left( (V')^* \frac{1}{\mathcal{U}^T} (V'')^T \right)_{\mathbf{R}_3, \mathbf{R}_2} \\
&\quad - \left( (V')^* \frac{1}{\mathcal{U}^T} (V'')^T \right)_{\mathbf{R}_3, \mathbf{R}_1} \left( (V')^* \frac{1}{\mathcal{U}^T} (V'')^T \right)_{\mathbf{R}_4, \mathbf{R}_2} \\
&\quad - \left( (V')^* \frac{1}{\mathcal{U}^T} (V'')^T \right)_{\mathbf{R}_1, \mathbf{R}_2} \left( (V')^* \frac{1}{\mathcal{U}^T} (V'')^T \right)_{\mathbf{R}_4, \mathbf{R}_3}.
\end{aligned}$$

To compute  $\langle \theta'' | H | \theta' \rangle / \langle \theta'' | \theta' \rangle$ , we use expression (B13), but replace  $\rho$  with

$$\bar{\rho}_{\ell_x, \ell_y, z, \sigma, z', \sigma'} = \sum_{\mathbf{K}, \mathbf{K}'} V'_{-\ell_x, -\ell_y, z', \sigma', \mathbf{K}'} \left( \frac{1}{\mathcal{U}} \right)_{\mathbf{K}', \mathbf{K}} (V'_{-\ell_x, -\ell_y, z, \sigma, \mathbf{K}})^* \quad (\text{C16})$$

and  $\kappa$  with

$$\bar{\kappa}_{\ell_x, \ell_y, z, \sigma, z', \sigma'} = \sum_{\mathbf{K}, \mathbf{K}'} U'_{-\ell_x, -\ell_y, z', \sigma', \mathbf{K}'} \left( \frac{1}{\mathcal{U}} \right)_{\mathbf{K}', \mathbf{K}} (V'_{-\ell_x, -\ell_y, z, \sigma, \mathbf{K}})^*. \quad (\text{C17})$$

#### APPENDIX D: FIXING THE ORDER PARAMETER PHASE ADDITIVE CONSTANT

Note that any self-consistent solution of the Bogoliubov–de Gennes equations remains a self-consistent solution under the transformation

$$\begin{aligned}
\Delta_{\mathbf{R}, \mathbf{R}'} &\rightarrow e^{i\xi} \Delta_{\mathbf{R}, \mathbf{R}'}, \\
U_{\mathbf{R}, \mathbf{K}} &\rightarrow e^{i\xi/2} U_{\mathbf{R}, \mathbf{K}}, \\
V_{\mathbf{R}, \mathbf{K}} &\rightarrow e^{-i\xi/2} U_{\mathbf{R}, \mathbf{K}},
\end{aligned}$$

where  $\xi$  is a real constant. Because  $Z \equiv (VU^{-1})^*$ , the ground state (A20) becomes

$$|0, \xi\rangle = \mathcal{N} \exp \left[ \frac{1}{2} \sum_{\mathbf{R}, \mathbf{R}'} e^{i\xi} c_{\mathbf{R}}^\dagger Z_{\mathbf{R}, \mathbf{R}'} c_{\mathbf{R}'}^\dagger \right] |\text{vac}\rangle. \quad (\text{D1})$$

Expanding the exponential, one sees that  $|0, \xi\rangle$  is a superposition

$$|0, \xi\rangle = \sum_{\mathbf{n}} e^{in\xi} |0, \mathbf{n}\rangle,$$

where  $|0, \mathbf{n}\rangle = \int_0^{2\pi} (d\xi/2\pi) e^{-in\xi} |0, \xi\rangle$  is an unnormalized state with  $\mathbf{n}$  total pairs ( $2\mathbf{n}$  total particles) in the system. Clearly,  $\xi$  shows up as the relative phase between states with different numbers of particles. If a superconducting system with a fixed number of pairs  $\bar{\mathbf{n}}$  is modeled using the Bogoliubov–de Gennes equations, the state of the system can be described by one of the terms in the sum, i.e.,  $|0, \bar{\mathbf{n}}\rangle / \sqrt{\langle 0, \bar{\mathbf{n}} | 0, \bar{\mathbf{n}} \rangle}$ . For mathematical convenience, we often calculate physical properties of the system using

the entire superposition  $|0, \xi\rangle$ . However, correct physical predictions about the system cannot depend on the value of  $\xi$ .

It is therefore jarring that adding a constant to the rescaled order parameter phase (6) does in fact alter the predictions of Eq. (8). Indeed, taking  $\Theta_{\mathbf{r}} \rightarrow \Theta_{\mathbf{r}} + \xi$  multiplies each  $c_{\mathbf{R}}^\dagger$  in Eq. (A25) by an extra factor of  $e^{i\theta\xi/2}$ . Comparing definition (D1), we see that  $|\theta\rangle$  has changed to  $|\theta, \theta\xi\rangle$ . If we expand

$$|\theta, \xi\theta\rangle = \sum_{\mathbf{n}} e^{in\theta\xi} |\theta, \mathbf{n}\rangle,$$

the matrix elements in Eq. (8) depend on  $\xi$  as

$$\begin{aligned}
\langle \theta, \theta\xi | \theta', \theta'\xi \rangle &= \sum_{\mathbf{n}} e^{in(\theta-\theta')\xi} \langle \theta, \mathbf{n} | \theta', \mathbf{n} \rangle, \\
\langle \theta, \theta\xi | H | \theta', \theta'\xi \rangle &= \sum_{\mathbf{n}} e^{in(\theta-\theta')\xi} \langle \theta, \mathbf{n} | H | \theta', \mathbf{n} \rangle.
\end{aligned} \quad (\text{D2})$$

In light of this expansion, one realizes that, for a system with a fixed number of pairs  $\bar{\mathbf{n}}$ , one would actually like to solve a modified version of Eq. (8) with fixed particle number

$$\sum_{\theta} \langle \theta, \bar{\mathbf{n}} | H | \theta', \bar{\mathbf{n}} \rangle \psi(\theta') = E \sum_{\theta} \langle \theta, \bar{\mathbf{n}} | \theta', \bar{\mathbf{n}} \rangle \psi(\theta'). \quad (\text{D3})$$

This equation does not depend on  $\xi$ , as required physically.

Nevertheless, the original Eq. (8) can be used provided that we choose a specific value of  $\xi$  satisfying

$$\begin{aligned}
\langle \theta, \theta\xi | \theta', \theta'\xi \rangle &\approx \frac{e^{i\bar{\mathbf{n}}(\theta-\theta')\xi} \langle \theta, \bar{\mathbf{n}} | \theta', \bar{\mathbf{n}} \rangle}{\sqrt{\langle \theta, \bar{\mathbf{n}} | \theta, \bar{\mathbf{n}} \rangle \langle \theta', \bar{\mathbf{n}} | \theta', \bar{\mathbf{n}} \rangle}} \\
&= \frac{e^{i\bar{\mathbf{n}}(\theta-\theta')\xi} \langle \theta, \bar{\mathbf{n}} | \theta', \bar{\mathbf{n}} \rangle}{\langle 0, \bar{\mathbf{n}} | 0, \bar{\mathbf{n}} \rangle}, \\
\langle \theta, \theta\xi | H | \theta', \theta'\xi \rangle &\approx \frac{e^{i\bar{\mathbf{n}}(\theta-\theta')\xi} \langle \theta, \bar{\mathbf{n}} | H | \theta', \bar{\mathbf{n}} \rangle}{\sqrt{\langle \theta, \bar{\mathbf{n}} | \theta, \bar{\mathbf{n}} \rangle \langle \theta', \bar{\mathbf{n}} | \theta', \bar{\mathbf{n}} \rangle}} \\
&= \frac{e^{i\bar{\mathbf{n}}(\theta-\theta')\xi} \langle \theta, \bar{\mathbf{n}} | H | \theta', \bar{\mathbf{n}} \rangle}{\langle 0, \bar{\mathbf{n}} | 0, \bar{\mathbf{n}} \rangle},
\end{aligned} \quad (\text{D4})$$

for  $\bar{\mathbf{n}}$  equal to the number of pairs in the system. If this condition is satisfied, Eq. (8) approximately reduces to Eq. (D3). To satisfy Eqs. (D4), in this paper we choose  $\xi$  such that Eq. (6) is an antisymmetric function of  $z$ , as in Fig. 1(c). This implies that  $e^{in(\theta-\theta')\xi} \langle \theta, \mathbf{n} | \theta', \mathbf{n} \rangle$  is real for all  $\mathbf{n}$ :

$$\begin{aligned}
(e^{in(\theta-\theta')\xi} \langle \theta, \mathbf{n} | \theta', \mathbf{n} \rangle)^* &= e^{-in\theta\xi} \langle -\theta, \mathbf{n} | -\theta', \mathbf{n} \rangle e^{in\theta'\xi} \\
&= e^{in\theta\xi} \langle \theta, \mathbf{n} | \hat{R}^\dagger \hat{R} | \theta', \mathbf{n} \rangle e^{-in\theta'\xi} \\
&= e^{in(\theta-\theta')\xi} \langle \theta, \mathbf{n} | \theta', \mathbf{n} \rangle.
\end{aligned}$$

In the second equality, we introduced an operator  $\hat{R}$  that takes  $z$  to  $-z$ , and we used the  $z \leftrightarrow -z$  reflection symmetry of the problem about the Josephson junction. The third



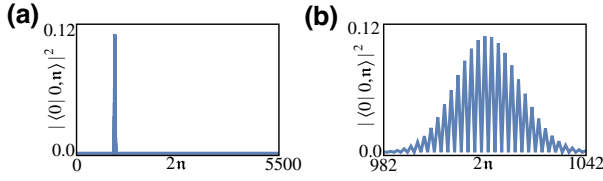


FIG. 5. (a) Plot of the overlap  $|\langle 0|0, n\rangle|^2$  versus the number of particles  $2n$  for the charge qubit parameters detailed in the main text. Strong peak is evident near  $2n = 1012$  particles. (b) Expanded plot in the range  $2n = 982$  to  $1042$  particles shows the shape of the peak.

equality uses the fact that two reflections  $\hat{R}^\dagger \hat{R}$  in succession produce an identity operation. Similarly, our choice of  $\xi$  ensures that  $e^{in(\theta-\theta')\xi} \langle \theta, n|H|\theta', n\rangle$  is real for all  $n$ :

$$\begin{aligned} (e^{in(\theta-\theta')\xi} \langle \theta, n|H|\theta', n\rangle)^* &= e^{in(-\theta+\theta')\xi} \langle -\theta, n|H^*|-\theta', n\rangle \\ &= e^{in(\theta-\theta')\xi} \langle \theta, n|\hat{R}^\dagger H^* \hat{R}|\theta', n\rangle \\ &= e^{in(\theta-\theta')\xi} \langle \theta, n|H|\theta', n\rangle. \end{aligned}$$

Now, numerically, we find that the terms in Eqs. (D2) are strongly peaked as a function of  $n$  about  $n = \bar{n}$ . A sample calculation, performed using the charge qubit parameters described in the main text, is shown in Fig. 5 for  $e^{in(\theta-\theta')\xi} \langle \theta, n|H|\theta', n\rangle$  in the case  $\theta = \theta' = 0$ . Since they are real and do not have a rapidly varying phase, the terms with  $n$  close to  $\bar{n}$  add constructively and determine the value of the sum. As a result, Eqs. (D4) are satisfied: we have numerically verified agreement to within about 1% for the overlap  $\langle \theta, \theta\xi|\theta', \theta'\xi\rangle$  and for the one-body operators in the Hamiltonian  $\langle \theta, \theta\xi|c_{\mathbf{R}}^\dagger c_{\mathbf{R}'}|\theta', \theta'\xi\rangle$  at a few choices of  $\theta$ ,  $\theta'$ ,  $\mathbf{R}$ , and  $\mathbf{R}'$ . [We expect that Eqs. (D4) would also be satisfied for the two-body operators in the Hamiltonian, but did not check this numerically.] Had we chosen  $\xi$  injudiciously, there would have been differences in phase leading to cancellations within the sums (D2). As a result, Eqs. (D4) would not be well satisfied.

Although this discussion has focused on the case of the charge qubit, analogous remarks apply to the rf-SQUID qubit. The rescaled phase function (15) is chosen so that it is antisymmetric on  $z$ , as shown in Fig. 2(c). This allows us to get physically relevant results by solving Eq. (17) without projecting on to states of fixed particle number.

## APPENDIX E: DEFINITION OF THE ORTHONORMAL BASIS

In the limit of large systems, the states  $|\theta\rangle$  approach orthonormality. This follows from the Onishi formula  $|\langle \theta|\theta'\rangle|^2 = \det \mathcal{U}$  in the limit in which matrix (9) becomes large. To solve Eq. (8) for a finite system, though, it is convenient to construct an orthonormal basis explicitly. Our nonorthonormal basis, defined in the main text, comprises

states  $|\theta\rangle$ , where  $-\theta_{\max} < \theta \leq \theta_{\max}$ . The value of  $\theta_{\max}$  is determined by  $|\theta\rangle = |\theta + 2\theta_{\max}\rangle$ ; based on Eq. (A25) a sufficient condition is

$$e^{i2\theta_{\max}(\Theta_{\mathbf{r}}+\Theta_{\mathbf{r}'})/2} = 1 \quad \text{for all } \mathbf{r} \text{ and } \mathbf{r}'. \quad (\text{E1})$$

For instance, if we have a charge qubit in which  $\Theta_{\mathbf{r}}/2$  changes from  $-1/4$  to  $1/4$  abruptly across the Josephson junction from one lattice site to the next then we have  $\theta_{\max} = 2\pi$ . If instead  $\Theta_{\mathbf{r}}/2$  changes from  $-1/4$  to  $1/4$  linearly over  $\Delta z$  lattice sites, with  $\Delta z$  referring to the thickness of the Josephson junction, then  $\theta_{\max} = 2\pi \Delta z$ .

We define orthonormal states  $|n\rangle$  as follows. Using expression (A25) for  $|\theta'\rangle$  and defining

$$\tilde{c}_{\mathbf{R}}^\dagger = e^{i\theta' \Theta_{\mathbf{R}}/2} c_{\mathbf{R}}^\dagger, \quad (\text{E2})$$

one sees that the overlap matrix elements satisfy  $\langle \theta|\theta'\rangle = \langle \theta - \theta'|0\rangle$ . Fourier transforming, we define  $o_n$  by

$$\begin{aligned} &\frac{1}{2\theta_{\max}} \int_{-\theta_{\max}}^{\theta_{\max}} d\theta e^{i\theta n} \frac{1}{2\theta_{\max}} \int_{-\theta_{\max}}^{\theta_{\max}} d\theta' e^{-i\theta' n'} \langle \theta - \theta'|0\rangle \\ &= \begin{cases} o_n, & n = n', \\ 0, & \text{otherwise,} \end{cases} \end{aligned} \quad (\text{E3})$$

where

$$n = 2\pi m/2\theta_{\max} \quad (\text{E4})$$

for  $m$  an integer in the range  $-M/2, \dots, M/2$  with  $M$  an even integer. It follows that the states

$$|n\rangle = \frac{1}{\sqrt{o_n}} \frac{1}{2\theta_{\max}} \int_{-\theta_{\max}}^{\theta_{\max}} d\theta e^{-i\theta n} |\theta\rangle \quad (\text{E5})$$

satisfy the orthonormality condition

$$\langle n|n'\rangle = \begin{cases} 1, & n = n', \\ 0, & \text{otherwise.} \end{cases} \quad (\text{E6})$$

Some eigenvalues  $o_n$  approach zero because the basis of  $|\theta\rangle$  states is overcomplete; we exclude the corresponding states  $|n\rangle$  from our basis.

Given the definition of  $|n\rangle$ , it is possible to perform a unitary transformation to a coarse-grained  $\bar{\theta}$  basis defined by an inverse Fourier transform over the valid  $|n\rangle$  states:

$$|\bar{\theta}\rangle = \sum_n e^{i\bar{\theta}n} |n\rangle / \sqrt{M+1}. \quad (\text{E7})$$

The number of such states is  $M+1$ , and they lie in value between  $-\theta_{\max}$  and  $\theta_{\max}$ , so their allowed values are  $\bar{\theta} = 2\theta_{\max}m/(M+1)$  with  $m = -M/2, \dots, M/2$  integral.

An upper bound on  $M$  is given by  $\theta_{\max} N_{\text{pairs}}/\pi$ , where  $N_{\text{pairs}}$  is the total number of pairs occupying the system. This estimate is obtained by applying the theorem of Bloch and Messiah to Eq. (A25). As noted previously, this theorem states that there are unitary matrices  $C$  and  $D$  for which  $\bar{U} = D^\dagger U C^\dagger$  and  $\bar{V} = D^T U C^\dagger$  are real and take simple block-diagonal forms. The matrix  $\bar{U}$  has  $2 \times 2$  blocks of the form  $u_{\mathbf{J}} \begin{bmatrix} 1 & 0 \\ 0 & 1 \end{bmatrix}$ , while these blocks take the form  $v_{\mathbf{J}} \begin{bmatrix} 0 & 1 \\ -1 & 0 \end{bmatrix}$  in the case of  $\bar{V}$ . Here, the  $2 \times 2$  block involving state  $\mathbf{J}$  involves a paired state that we label  $\bar{\mathbf{J}}$ . Defining

$$d_{\mathbf{J}}^\dagger = \sum_{\mathbf{R}} c_{\mathbf{R}}^\dagger e^{i\theta_{\mathbf{R}}/2} D_{\mathbf{R},\mathbf{J}}, \quad (\text{E8})$$

we find that  $\frac{1}{2} \sum_{\mathbf{R},\mathbf{R}'} e^{i\theta(\Theta_{\mathbf{R}}+\Theta_{\mathbf{R}'})/2} c_{\mathbf{R}}^\dagger Z_{\mathbf{R},\mathbf{R}'} c_{\mathbf{R}'}^\dagger = \sum_{\mathbf{J}} d_{\mathbf{J}}^\dagger (v_{\mathbf{J}}/u_{\mathbf{J}}) d_{\mathbf{J}}^\dagger$ . Inserting this into Eq. (A25) yields

$$|\theta\rangle = \mathcal{N} \exp\left(\sum_{\mathbf{J}} d_{\mathbf{J}}^\dagger \frac{v_{\mathbf{J}}}{u_{\mathbf{J}}} d_{\mathbf{J}}^\dagger\right) |\text{vac}\rangle$$

$$\begin{aligned} &= \mathcal{N} \prod_{\mathbf{J}} \left(1 + d_{\mathbf{J}}^\dagger \frac{v_{\mathbf{J}}}{u_{\mathbf{J}}} d_{\mathbf{J}}^\dagger\right) |\text{vac}\rangle \\ &\approx \mathcal{N} \prod_{\mathbf{J} \sim \text{Fermi sea}} \left(1 + d_{\mathbf{J}}^\dagger \frac{v_{\mathbf{J}}}{u_{\mathbf{J}}} d_{\mathbf{J}}^\dagger\right) |\text{vac}\rangle \\ &= \mathcal{N} \left(1 + \sum_{\mathbf{J} \sim \text{Fermi sea}} d_{\mathbf{J}}^\dagger \frac{v_{\mathbf{J}}}{u_{\mathbf{J}}} d_{\mathbf{J}}^\dagger \right. \\ &\quad \left. + \dots + \prod_{\mathbf{J} \sim \text{Fermi sea}} d_{\mathbf{J}}^\dagger \frac{v_{\mathbf{J}}}{u_{\mathbf{J}}} d_{\mathbf{J}}^\dagger\right) |\text{vac}\rangle. \quad (\text{E9}) \end{aligned}$$

The notation  $\mathbf{J} \sim \text{Fermi sea}$  indicates states that are within the Fermi sea or not too far above the Fermi surface. The approximate equality in the third line uses that fact that high-energy states well above the Fermi surface have  $v_{\mathbf{J}} \rightarrow 0$ . The final equality comes from multiplying out the product into a sum of terms. Inserting this expression into Eq. (E5) yields

$$\begin{aligned} |n\rangle &\approx \frac{\mathcal{N}}{\sqrt{\mathcal{O}_n}} \frac{1}{2\theta_{\max}} \int_{-\theta_{\max}}^{\theta_{\max}} d\theta e^{-in\theta} \left(1 + \dots + \prod_{\mathbf{J} \sim \text{Fermi Sea}} d_{\mathbf{J}}^\dagger \frac{v_{\mathbf{J}}}{u_{\mathbf{J}}} d_{\mathbf{J}}^\dagger\right) |\text{vac}\rangle \\ &= \frac{\mathcal{N}}{\sqrt{\mathcal{O}_n}} \frac{1}{2\theta_{\max}} \int_{-\theta_{\max}}^{\theta_{\max}} d\theta e^{-in\theta} \left(1 + \dots + \prod_{\mathbf{J} \sim \text{Fermi sea}} \sum_{\mathbf{R},\mathbf{R}'} c_{\mathbf{R}}^\dagger e^{i\theta_{\mathbf{R}}/2} D_{\mathbf{R},\mathbf{J}} \frac{v_{\mathbf{J}}}{u_{\mathbf{J}}} c_{\mathbf{R}'}^\dagger e^{i\theta_{\mathbf{R}'}/2} D_{\mathbf{R}',\bar{\mathbf{J}}}\right) |\text{vac}\rangle, \quad (\text{E10}) \end{aligned}$$

where Eq. (E8) has been used in the final line. If  $n$  is too large, the right-hand side will vanish. To see this, note that

$$\frac{1}{2\theta_{\max}} \int_{-\theta_{\max}}^{\theta_{\max}} d\theta e^{-in\theta} e^{i\theta(\Theta_{\mathbf{r}_1} + \dots + \Theta_{\mathbf{r}_{2T}})/2} = \begin{cases} 1, & n = (\Theta_{\mathbf{r}_1} + \dots + \Theta_{\mathbf{r}_{2T}})/2, \\ 0, & \text{otherwise,} \end{cases} \quad (\text{E11})$$

using Eq. (E1). Assuming that  $\Theta_{\mathbf{r}}$  is at most  $1/2$ , the largest possible value of  $(\Theta_{\mathbf{r}_1} + \dots + \Theta_{\mathbf{r}_{2T}})/2$  is  $T/2$ ; the Kronecker delta then enforces  $n = T/2$ . Thus, the largest possible value of  $n$  that could possibly give a nonvanishing result for Eq. (E10) is  $n = N_{\text{pairs}}/2$ , where  $N_{\text{pairs}}$  is the number of occupied pairs appearing in  $\prod_{\mathbf{J} \sim \text{Fermi sea}}$ . Similarly, the smallest possible value of  $n$  is  $-N_{\text{pairs}}/2$ . Given Eq. (E4), we find that  $2\pi(M/2)/2\theta_{\max} \leq N_{\text{pairs}}/2$ , or  $M \leq N_{\text{pairs}}\theta_{\max}/\pi$  as claimed above.

In the case of a charge qubit composed of two weakly coupled superconducting islands with a relatively abrupt phase change, as in Fig. 1(c), we can find a better estimate of  $M + 1$ . The basis size  $M + 1$  turns out to scale as the number of pairs  $N_{\text{shared}}$  in  $|\theta\rangle$  that are shared on both islands, which is roughly the number of pairs near the chemical potential of the system. To show this, we write

$$\begin{aligned} |\theta\rangle &= \mathcal{N} \prod_{\mathbf{J} \sim \text{Fermi sea}} \left(1 + d_{\mathbf{J}}^\dagger \frac{v_{\mathbf{J}}}{u_{\mathbf{J}}} d_{\mathbf{J}}^\dagger\right) |\text{vac}\rangle = \mathcal{N} \prod_{\mathbf{J} \text{ left}} \left(1 + d_{\mathbf{J}}^\dagger \frac{v_{\mathbf{J}}}{u_{\mathbf{J}}} d_{\mathbf{J}}^\dagger\right) \prod_{\mathbf{J} \text{ right}} \left(1 + d_{\mathbf{J}}^\dagger \frac{v_{\mathbf{J}}}{u_{\mathbf{J}}} d_{\mathbf{J}}^\dagger\right) \prod_{\mathbf{J} \text{ shared}} \left(1 + d_{\mathbf{J}}^\dagger \frac{v_{\mathbf{J}}}{u_{\mathbf{J}}} d_{\mathbf{J}}^\dagger\right) |\text{vac}\rangle \\ &\approx \mathcal{N}' \prod_{\mathbf{J} \text{ left}} d_{\mathbf{J}}^\dagger d_{\mathbf{J}}^\dagger \prod_{\mathbf{J} \text{ right}} d_{\mathbf{J}}^\dagger d_{\mathbf{J}}^\dagger \prod_{\mathbf{J} \text{ shared}} \left(1 + d_{\mathbf{J}}^\dagger \frac{v_{\mathbf{J}}}{u_{\mathbf{J}}} d_{\mathbf{J}}^\dagger\right) |\text{vac}\rangle, \quad (\text{E12}) \end{aligned}$$

where  $\mathbf{J}$  left and  $\mathbf{J}$  right refer to states that are localized well within the Fermi sea of the left or right island, respectively. These states have  $v_J/u_J$  very large, permitting the final approximate equality. Let  $N_{\text{left}}$  be the number of pairs in the  $\mathbf{J}$  left product,  $N_{\text{right}}$  be the number of pairs in the  $\mathbf{J}$  right product, and  $N_{\text{shared}}$  be the number of pairs in the  $\mathbf{J}$  shared product. We are considering the case of an abrupt phase change, in which the electrons in the system have  $\Theta_{\mathbf{R}} = -1/2$  or  $1/2$  depending on whether they inhabit the left island or the right island. Thus, when we calculate Eq. (E10), the integrals take the form

$$\frac{1}{2\theta_{\text{max}}} \int_{-\theta_{\text{max}}}^{\theta_{\text{max}}} d\theta e^{-in\theta} e^{i\theta(N_{\text{right}}-N_{\text{left}})/2} e^{i\theta(\Theta_{\mathbf{r}_1}+\dots+\Theta_{\mathbf{r}_{2T}})/2}$$

with the largest possible value of  $T$  given by the number of pairs  $N_{\text{shared}}$  that can wander from the left island to the right island. We see that  $n$  ranges from  $(N_{\text{right}} - N_{\text{left}})/2 - N_{\text{shared}}/2$  to  $(N_{\text{right}} - N_{\text{left}})/2 + N_{\text{shared}}/2$ . Recalling Eq. (E4), we see that the size of the basis is determined by  $2\pi(M/2)/2\theta_{\text{max}} \leq N_{\text{shared}}/2$ , so that  $M \leq N_{\text{shared}}\theta_{\text{max}}/\pi$ . Physically,  $|n\rangle$  is a state with  $2n$  more pairs on the right island than on the left island.

The construction of an orthonormal basis for Eq. (17) closely parallels the construction for Eq. (8). In the limit of large systems, the states  $|\odot, \theta\rangle$  and  $|\ominus, \theta\rangle$  approach orthonormality. For smaller systems, we construct an orthonormal basis explicitly as follows. The original nonorthogonal basis is composed of  $|\odot, \theta\rangle$  and  $|\ominus, \theta\rangle$  with  $-\theta_{\text{max}} < \theta \leq \theta_{\text{max}}$  and  $\theta_{\text{max}}$  fixed by Eq. (E1). For an rf-SQUID qubit,  $\theta_{\text{max}}$  will approach  $2\pi N_z$ , with  $N_z$  the number of sites around the circumference of the system. This greatly exceeds the value of  $\theta_{\text{max}}$  in the charge qubit case, consistent with the fact that  $\theta$  is unbounded in LE theory in the case of an rf SQUID. The overlap matrix is composed of  $2 \times 2$  blocks

$$\begin{aligned} & \begin{bmatrix} \langle \odot, \theta | \odot, \theta' \rangle & \langle \odot, \theta | \ominus, \theta' \rangle \\ \langle \odot, \theta | \ominus, \theta' \rangle & \langle \ominus, \theta | \ominus, \theta' \rangle \end{bmatrix} \\ &= \begin{bmatrix} \langle \odot, \theta - \theta' | \odot, 0 \rangle & \langle \odot, \theta - \theta' | \ominus, 0 \rangle \\ \langle \odot, \theta - \theta' | \odot, 0 \rangle & \langle \odot, \theta - \theta' | \ominus, 0 \rangle \end{bmatrix} \end{aligned} \quad (\text{E13})$$

for  $-\theta_{\text{max}} < \theta, \theta' \leq \theta_{\text{max}}$ . After a Fourier transform, the overlap matrix becomes block diagonal with  $2 \times 2$  blocks of the form

$$\begin{aligned} & \int_{-\theta_{\text{max}}}^{\theta_{\text{max}}} d\theta \int_{-\theta_{\text{max}}}^{\theta_{\text{max}}} d\theta' \frac{e^{i\theta n - i\theta' n'}}{(2\theta_{\text{max}})^2} \begin{bmatrix} \langle \odot, \theta | \odot, \theta' \rangle & \langle \odot, \theta | \ominus, \theta' \rangle \\ \langle \odot, \theta | \ominus, \theta' \rangle & \langle \ominus, \theta | \ominus, \theta' \rangle \end{bmatrix} \\ &= \begin{cases} O_n, & n = n', \\ 0, & \text{otherwise,} \end{cases} \end{aligned} \quad (\text{E14})$$

where  $O_n$  is a  $2 \times 2$  matrix and  $n, n'$  satisfy (E4). The eigenvalues of  $O_n$ , labeled  $o_{1,n}$  and  $o_{2,n}$ , have corresponding eigenvectors

$$O_n \begin{bmatrix} a_{i,n} \\ b_{i,n} \end{bmatrix} = o_{i,n} \begin{bmatrix} a_{i,n} \\ b_{i,n} \end{bmatrix}$$

for  $i = 1, 2$ . We can define orthonormal states in terms of these eigenvectors by

$$|i, n\rangle = \frac{1}{\sqrt{o_{i,n}}} \frac{1}{2\theta_{\text{max}}} \int_{-\theta_{\text{max}}}^{\theta_{\text{max}}} d\theta e^{-i\theta n} (a_{i,n} |\odot, \theta\rangle + b_{i,n} |\ominus, \theta\rangle) \quad (\text{E15})$$

for  $i = 1, 2$ . They satisfy

$$\langle i, n | i', n' \rangle = \begin{cases} 1, & i = i' \text{ and } n = n', \\ 0, & \text{otherwise.} \end{cases} \quad (\text{E16})$$

Because the original nonorthogonal basis is overcomplete, some eigenvalues  $o_{i,n}$  approach zero; the corresponding states  $|i, n\rangle$  are omitted from our basis. We denote by  $2(M+1)$  the number of valid orthogonal basis states  $|i, n\rangle$ .

Given this definition of  $|i, n\rangle$ , it is possible to perform a unitary transformation to a coarse-grained phase basis defined by an inverse Fourier transform over the valid  $|i, n\rangle$  states:

$$|i, \bar{\theta}\rangle = \sum_{n=-M/2}^{M/2} e^{i\bar{\theta}n} |i, n\rangle / \sqrt{M+1}. \quad (\text{E17})$$

Since the number of such states for a given  $i$  is  $M+1$ , the spacing between them is  $\Delta\bar{\theta} = 2\theta_{\text{max}}/(M+1)$ . As  $M+1$  grows with system size, this spacing shrinks to zero.

Applying the theorem of Bloch and Messiah as above to  $|\odot, \theta\rangle$  and  $|\ominus, \theta\rangle$ , we can argue that a rough upper bound on  $M+1$  is given by the number of occupied pairs in the system. It is important to emphasize that the quantum number  $n$  in  $|i, n\rangle$  does not admit a simple interpretation in terms of the positions of Cooper pairs in the system.

## APPENDIX F: DERIVATION OF THE LUMPED-ELEMENT EQUATIONS

In the coarse-grained  $\bar{\theta}$  basis, the Schrödinger equation (8) becomes an  $(M+1) \times (M+1)$  matrix equation

$$\sum_{\bar{\theta}'} \langle \bar{\theta} | \mathcal{H} | \bar{\theta}' \rangle \psi(\bar{\theta}') = E \psi(\bar{\theta}), \quad (\text{F1})$$

where

$$\begin{aligned} \langle \bar{\theta} | \mathcal{H} | \bar{\theta}' \rangle &= \frac{1}{M+1} \frac{1}{(2\theta_{\max})^2} \sum_{n=-M/2}^{M/2} \frac{e^{-i\bar{\theta}n}}{\sqrt{O_n}} \int_{-\theta_{\max}}^{\theta_{\max}} d\theta e^{i\theta n} \\ &\sum_{n'=-M/2}^{M/2} \frac{e^{i\bar{\theta}'n'}}{\sqrt{O_{n'}}} \int_{-\theta_{\max}}^{\theta_{\max}} d\theta e^{-i\theta'n'} \langle \theta | H | \theta' \rangle. \end{aligned} \quad (\text{F2})$$

As the size of the system, and the basis size  $M+1$ , grows, the overlap matrix elements  $\langle \theta | \theta' \rangle$  decay rapidly for  $\theta \neq \theta'$  as a consequence of Eq. (9). The original  $|\theta\rangle$  basis tends toward orthonormality, and one expects the orthonormal basis  $|\bar{\theta}\rangle$  that we constructed to approach  $|\theta\rangle|_{\theta=\bar{\theta}}$ , the original basis state with  $\theta$  evaluated at  $\bar{\theta}$ . Thus, in this limit we approximate  $\langle \bar{\theta} | \mathcal{H} | \bar{\theta}' \rangle \approx \langle \theta | H | \theta' \rangle|_{\theta=\bar{\theta}, \theta'=\bar{\theta}'}$ . Recall decomposition (1),  $\langle \theta | H | \theta' \rangle = \langle \theta | T + P + W | \theta' \rangle$ . Employing Eq. (E2), we can show that the potential and interaction energies satisfy  $\langle \theta | P + W | \theta' \rangle = \langle \theta - \theta' | P + W | 0 \rangle$ . Therefore, along the diagonal of the Hamiltonian matrix in Eq. (F1),  $\langle \theta | P + W | \theta \rangle = \langle 0 | P + W | 0 \rangle$  contributes an overall constant that simply shifts  $E$  in Eq. (F1). Only  $\langle \theta | T | \theta \rangle$  depends upon  $\theta$ ; this dependence is physically important and should not be neglected. However, in the off-diagonal elements, we approximate  $\langle \theta | T | \theta' \rangle$  as  $\langle \theta - \theta' | T | 0 \rangle$ , which is reasonable if the error incurred thereby is small:  $|\langle \theta - \theta' | T | 0 \rangle - \langle \theta | T | \theta' \rangle| \ll |\langle \theta - \theta' | T + P + W | 0 \rangle|$ . Summarizing, we have

$$\begin{aligned} \langle \bar{\theta} | \mathcal{H} | \bar{\theta}' \rangle &\approx \delta_{\bar{\theta}, \bar{\theta}'} (\langle \theta | T | \theta \rangle - \langle 0 | T | 0 \rangle)|_{\theta=\bar{\theta}, \theta'=\bar{\theta}'} \\ &+ \langle \theta - \theta' | T + P + W | 0 \rangle|_{\theta=\bar{\theta}, \theta'=\bar{\theta}'}. \end{aligned} \quad (\text{F3})$$

Clearly, the first line is diagonal in the phase basis. The second line, since it depends only on  $\theta - \theta'$ , becomes diagonal in the basis of  $|n\rangle$  states (E5).

We can develop the analysis further in the case of a charge qubit composed of two weakly coupled superconducting islands with a relatively abrupt phase change, as in Fig. 1(c). The matrix element of the tunneling Hamiltonian is

$$\begin{aligned} \langle \theta | T | \theta' \rangle &= -\langle \theta - \theta' | \sum_{\mathbf{R}} \sum_{\mathbf{a}=\pm\mathbf{a}_x, \pm\mathbf{a}_y, \pm\mathbf{a}_z} t_{\mathbf{r}+\mathbf{a}, \mathbf{r}} e^{i\theta'(\Theta_{\mathbf{r}} - \Theta_{\mathbf{r}+\mathbf{a}})/2} \\ &c_{\mathbf{r}+\mathbf{a}, \sigma}^\dagger c_{\mathbf{r}, \sigma} | 0 \rangle, \end{aligned} \quad (\text{F4})$$

where we have used Eq. (E2). It is useful to decompose  $T = T_{\text{near}} + T_{\text{far}}$ , where  $T_{\text{near}}$  contains the small fraction of terms in which  $\mathbf{r}$  is right near the junction and  $T_{\text{far}}$  contains all other tunneling terms. As a result of the form of Fig. 1(c), far from the junction,  $\Theta_{\mathbf{r}} \approx \Theta_{\mathbf{r}+\mathbf{a}}$ , so that  $e^{i\theta'(\Theta_{\mathbf{r}} - \Theta_{\mathbf{r}+\mathbf{a}})/2} \approx 1$ . Equation (F4) then implies that  $\langle \theta | T_{\text{far}} | \theta' \rangle \approx \langle \theta - \theta' | T_{\text{far}} | 0 \rangle$ . So, neglecting the contribution of  $T_{\text{near}}$ , we conclude that  $T_{\text{far}} + P + W$  is diagonal in basis (E5). A reasonable approximation is  $\langle n | T_{\text{far}} | n' \rangle = E_{\text{seas}} n^2 \delta_{n, n'}$ ,  $\langle n | W | n' \rangle = 4E_C n^2 \delta_{n, n'}$ , and

$\langle n | P | n' \rangle = -\tilde{\mu} n \delta_{n, n'}$ . Here,  $\tilde{\mu}$  denotes the electrochemical potential difference between the islands. The capacitive energy,  $4E_C = (2e)^2/2C$  in terms of an appropriate capacitance  $C$ , is familiar from LE theory. The unfamiliar coefficient  $E_{\text{seas}}$  is determined by the total energy of the two Fermi seas residing in the two superconducting islands. For simplicity, assume that each of the islands has volume  $L^3$ . Let the total number of electrons in the system be  $2N_{\text{tot}}$ , with  $N_{\text{tot}} + 2n$  residing on one island and  $N_{\text{tot}} - 2n$  residing on the other island. Then total energy of the two Fermi seas is  $\frac{3}{5} \hbar^2/2mL^2 (3\pi^2)^{2/3} ((N_{\text{tot}} + 2n)^{5/3} + (N_{\text{tot}} - 2n)^{5/3})$ . Taylor expanding this expression to second order, we deduce that  $E_{\text{seas}} = \hbar^2/2mL^2 (3\pi^2)^{2/3} \frac{8}{3} N_{\text{tot}}^{-1/3} = 8E_F/3N_{\text{tot}}$ , where  $E_F$  is the Fermi energy of each island when  $n = 0$ . For physical devices,  $E_{\text{seas}}$  is much smaller than  $4E_C$ . However, in simulations such as that performed in the text, where the Coulomb interaction is replaced with a short-range Hubbard interaction,  $E_{\text{seas}}$  becomes the important energy.

The contribution of  $T_{\text{near}}$  to the diagonal matrix elements takes the form  $\langle \theta | T_{\text{near}} | \theta \rangle \approx -E_J \cos \theta/2$ . Here, we have introduced the parameter  $E_J$  and used the fact that  $\Theta_{\mathbf{r}} - \Theta_{\mathbf{r}+\mathbf{a}} \approx 1$  when  $\mathbf{r}$  and  $\mathbf{r} + \mathbf{a}$  stand on opposite sides of the junction, implying that  $e^{i\theta'(\Theta_{\mathbf{r}} - \Theta_{\mathbf{r}+\mathbf{a}})/2} \approx e^{i\theta'/2}$  in Eq. (F4).

Assembling these results, we make a continuum approximation to our matrix equation (F1) for  $M+1$  large, obtaining the lumped-element equation

$$\begin{aligned} 4E_C \left( -i \frac{d}{d\bar{\theta}} - n_0 \right)^2 \psi(\bar{\theta}) \\ + E_J \left( 1 - \cos \frac{\bar{\theta}}{2} \right) \psi(\bar{\theta}) = E \psi(\bar{\theta}), \end{aligned} \quad (\text{F5})$$

where  $n_0 = \tilde{\mu}/8E_C$ . This should be compared with the standard lumped-element expression (14). There is a factor of 2 difference in the potential stemming from the fact that  $-\pi < \bar{\theta} \leq 2\pi$  in our theory. Setting  $\bar{\theta} = \tilde{\theta}/2$ ,  $\tilde{E}_C = E_C/4$ , and  $\tilde{n}_0 = 2n_0$ , we have

$$4\tilde{E}_C \left( -i \frac{d}{d\tilde{\theta}} - \tilde{n}_0 \right)^2 \psi(\tilde{\theta}) + E_J (1 - \cos \tilde{\theta}) \psi(\tilde{\theta}) = E \psi(\tilde{\theta}) \quad (\text{F6})$$

with  $-\pi < \tilde{\theta} \leq \pi$ . This agrees with Eq. (14).

We can make a similar argument in the case of an rf-SQUID qubit. The transformation to the orthogonal basis changes Eq. (17) to the matrix equation

$$\begin{aligned} \sum_{\bar{\theta}'} \begin{bmatrix} \langle 1, \bar{\theta} | \mathcal{H} | 1, \bar{\theta}' \rangle & \langle 1, \bar{\theta} | \mathcal{H} | 2, \bar{\theta}' \rangle \\ \langle 2, \bar{\theta} | \mathcal{H} | 1, \bar{\theta}' \rangle & \langle 2, \bar{\theta} | \mathcal{H} | 2, \bar{\theta}' \rangle \end{bmatrix} \begin{bmatrix} \psi(1, \bar{\theta}') \\ \psi(2, \bar{\theta}') \end{bmatrix} \\ = E \begin{bmatrix} \psi(1, \bar{\theta}) \\ \psi(2, \bar{\theta}) \end{bmatrix}, \end{aligned}$$

where  $\langle i, \bar{\theta} | \mathcal{H} | i', \bar{\theta}' \rangle$  satisfies a definition analogous to Eq. (F2):

$$\begin{aligned} \langle i, \bar{\theta} | \mathcal{H} | i', \bar{\theta}' \rangle &= \frac{1}{M+1} \frac{1}{(2\theta_{\max})^2} \sum_{n=-M/2}^{M/2} \frac{e^{-i\bar{\theta}n}}{\sqrt{O_n}} \int_{-\theta_{\max}}^{\theta_{\max}} d\theta e^{i\theta n} \sum_{n'=-M/2}^{M/2} \frac{e^{i\bar{\theta}'n'}}{\sqrt{O_{n'}}} \int_{-\theta_{\max}}^{\theta_{\max}} d\theta' e^{-i\theta'n'} \\ &\times \begin{bmatrix} a_{i,n} \\ b_{i,n} \end{bmatrix}^\dagger \begin{bmatrix} \langle \circlearrowleft, \theta | H | \circlearrowleft, \theta' \rangle & \langle \circlearrowleft, \theta | H | \circlearrowright, \theta' \rangle \\ \langle \circlearrowright, \theta | H | \circlearrowleft, \theta' \rangle & \langle \circlearrowright, \theta | H | \circlearrowright, \theta' \rangle \end{bmatrix} \begin{bmatrix} a_{i',n'} \\ b_{i',n'} \end{bmatrix}. \end{aligned} \quad (\text{F7})$$

For large systems, the overlap matrix (E13) tends to that of an orthonormal set of states, so we can approximate  $|1, \bar{\theta}\rangle = |\circlearrowleft, \theta\rangle|_{\theta=\bar{\theta}}$  and  $|2, \bar{\theta}\rangle = |\circlearrowright, \theta\rangle|_{\theta=\bar{\theta}}$ . Then, our matrix equation becomes

$$\sum_{\bar{\theta}'} \begin{bmatrix} \langle \circlearrowleft, \theta | H | \circlearrowleft, \theta' \rangle & \langle \circlearrowleft, \theta | H | \circlearrowright, \theta' \rangle \\ \langle \circlearrowright, \theta | H | \circlearrowleft, \theta' \rangle & \langle \circlearrowright, \theta | H | \circlearrowright, \theta' \rangle \end{bmatrix} \Big|_{\theta=\bar{\theta}, \theta'=\bar{\theta}'} \begin{bmatrix} \psi(\circlearrowleft, \bar{\theta}') \\ \psi(\circlearrowright, \bar{\theta}') \end{bmatrix} = E \begin{bmatrix} \psi(\circlearrowleft, \bar{\theta}) \\ \psi(\circlearrowright, \bar{\theta}) \end{bmatrix}. \quad (\text{F8})$$

The potential and interaction matrix elements satisfy

$$\begin{aligned} &\begin{bmatrix} \langle \circlearrowleft, \theta | P + W | \circlearrowleft, \theta' \rangle & \langle \circlearrowleft, \theta | P + W | \circlearrowright, \theta' \rangle \\ \langle \circlearrowright, \theta | P + W | \circlearrowleft, \theta' \rangle & \langle \circlearrowright, \theta | P + W | \circlearrowright, \theta' \rangle \end{bmatrix} \\ &= \begin{bmatrix} \langle \circlearrowleft, \theta - \theta' | P + W | \circlearrowleft, 0 \rangle & \langle \circlearrowleft, \theta - \theta' | P + W | \circlearrowright, 0 \rangle \\ \langle \circlearrowright, \theta - \theta' | P + W | \circlearrowleft, 0 \rangle & \langle \circlearrowright, \theta - \theta' | P + W | \circlearrowright, 0 \rangle \end{bmatrix}, \end{aligned}$$

which can be verified using a substitution like Eq. (E2).

For  $\theta \neq \theta'$ , we adopt the approximation

$$\begin{bmatrix} \langle \circlearrowleft, \theta | T | \circlearrowleft, \theta' \rangle & \langle \circlearrowleft, \theta | T | \circlearrowright, \theta' \rangle \\ \langle \circlearrowright, \theta | T | \circlearrowleft, \theta' \rangle & \langle \circlearrowright, \theta | T | \circlearrowright, \theta' \rangle \end{bmatrix} \approx \begin{bmatrix} \langle \circlearrowleft, \theta - \theta' | T | \circlearrowleft, 0 \rangle & \langle \circlearrowleft, \theta - \theta' | T | \circlearrowright, 0 \rangle \\ \langle \circlearrowright, \theta - \theta' | T | \circlearrowleft, 0 \rangle & \langle \circlearrowright, \theta - \theta' | T | \circlearrowright, 0 \rangle \end{bmatrix}$$

for the tunneling matrix elements. This relies on the approximation  $e^{i\theta'(\Theta_{\mathbf{r}} - \Theta_{\mathbf{r}+\mathbf{a}})/2} \approx 1$ , which is roughly true since  $\Theta_{\mathbf{r}}$  changes gradually along the long circumference of the rf-SQUID qubit [see Fig. 2(c)]. When  $\theta = \theta'$ , on the diagonal of the Hamiltonian matrix, we retain the explicit  $\theta$  dependence seen in the double-well potential in Fig. 2(d). This leads to

$$\begin{aligned} &\begin{bmatrix} \langle 1, \bar{\theta} | \mathcal{H} | 1, \bar{\theta}' \rangle & \langle 1, \bar{\theta} | \mathcal{H} | 2, \bar{\theta}' \rangle \\ \langle 2, \bar{\theta} | \mathcal{H} | 1, \bar{\theta}' \rangle & \langle 2, \bar{\theta} | \mathcal{H} | 2, \bar{\theta}' \rangle \end{bmatrix} \\ &\approx \delta_{\theta, \theta'} \begin{bmatrix} \langle \circlearrowleft, \theta | T | \circlearrowleft, \theta \rangle - \langle \circlearrowleft, 0 | T | \circlearrowleft, 0 \rangle & \langle \circlearrowleft, \theta | T | \circlearrowright, \theta \rangle - \langle \circlearrowleft, 0 | T | \circlearrowright, 0 \rangle \\ \langle \circlearrowright, \theta | T | \circlearrowleft, \theta \rangle - \langle \circlearrowright, 0 | T | \circlearrowleft, 0 \rangle & \langle \circlearrowright, \theta | T | \circlearrowright, \theta \rangle - \langle \circlearrowright, 0 | T | \circlearrowright, 0 \rangle \end{bmatrix} \Big|_{\theta=\bar{\theta}, \theta'=\bar{\theta}'} \\ &+ \begin{bmatrix} \langle \circlearrowleft, \theta - \theta' | T + P + W | \circlearrowleft, 0 \rangle & \langle \circlearrowleft, \theta - \theta' | T + P + W | \circlearrowright, 0 \rangle \\ \langle \circlearrowright, \theta - \theta' | T + P + W | \circlearrowleft, 0 \rangle & \langle \circlearrowright, \theta - \theta' | T + P + W | \circlearrowright, 0 \rangle \end{bmatrix} \Big|_{\theta=\bar{\theta}, \theta'=\bar{\theta}'} \end{aligned} \quad (\text{F9})$$

In the first term on the right-hand side, we approximate

$$\begin{aligned} \langle \circlearrowleft, \theta | T | \circlearrowleft, \theta \rangle - \langle \circlearrowleft, 0 | T | \circlearrowleft, 0 \rangle &= -E_J \cos \frac{1}{2}(\theta - \theta^\circ) + \frac{1}{2}E_L(\theta - \theta^\circ)^2, \\ \langle \circlearrowright, \theta | T | \circlearrowright, \theta \rangle - \langle \circlearrowright, 0 | T | \circlearrowright, 0 \rangle &= -E_J \cos \frac{1}{2}(\theta - \theta^\circ) + \frac{1}{2}E_L(\theta - \theta^\circ)^2. \end{aligned}$$

In each equation, the contribution proportional to  $E_L$  comes from tunneling terms in Eq. (2) distant from the Josephson junction, while the contribution proportional to  $E_J$  comes from tunneling through the Josephson junction.

The third line of Eq. (F9) depends only on  $\theta - \theta'$ . It therefore simplifies in basis (E15). As the system size grows and the overlap matrix (E13) tends to that of an orthonormal set of states, matrix  $O_n$  becomes nearly diagonal: its eigenvectors tend to  $a_{i,n} = 1$ ,  $b_{i,n} = 0$  and  $a_{i,n} = 0$ ,  $b_{i,n} = 1$ . Considering expression (E15), it becomes reasonable to adopt the notation  $|\circlearrowleft, n\rangle = |1, n\rangle$  and  $|\circlearrowright, n\rangle = |2, n\rangle$ . In this basis, the third line of Eq. (F9) is block diagonal with  $2 \times 2$  blocks



$$\begin{bmatrix} E_{\odot,n;\odot,n} & E_{\odot,n;\odot,n} \\ E_{\odot,n;\odot,n} & E_{\odot,n;\odot,n} \end{bmatrix}. \quad (\text{F10})$$

Now, the matrix elements in the third line of Eq. (F9) can be assumed real since one can introduce phases if necessary into the state definitions. (It is true that conditions such as  $|\odot, \theta_{\max}\rangle = |\odot, -\theta_{\max}\rangle$  could prevent the introduction of such phases consistently for all  $\theta - \theta'$  in Eq. (F9). However, since  $\theta_{\max}$  is so large for an rf-SQUID qubit, states such as  $|\odot, \theta_{\max}\rangle$  have extremely high energy and play no role in the accessible energy eigenstates of the system. Therefore, the matrix elements in the third line of Eq. (F9) can be written as a real part plus a correction that vanishes for energetically accessible states.) Because the third line of Eq. (F9) should decay with  $|\theta - \theta'|$ , we make a tight-binding approximation, retaining neighbors with  $\theta - \theta'|_{\theta=\bar{\theta},\theta'=\bar{\theta}'} = 0, \pm\Delta\bar{\theta}$ . [Recall that  $\Delta\bar{\theta} = 2\theta_{\max}/(M+1)$  as argued after Eq. (E17).] Then, each of the four functions in Eq. (F10) equals a constant plus a term proportional to  $\cos n\Delta\bar{\theta}$ . As system size increases and  $\Delta\bar{\theta}$  shrinks, we can truncate the cosine at second order to obtain

$$\begin{bmatrix} E_{\odot} & \\ & E_{\odot} \end{bmatrix} + \begin{bmatrix} E_{\odot;\odot} & E_{\odot;\odot} \\ E_{\odot;\odot} & E_{\odot;\odot} \end{bmatrix} n^2. \quad (\text{F11})$$

This result may be reminiscent of the energy proportional to  $n^2$  obtained in the case of a charge qubit with an abrupt junction, where  $|n\rangle$  is a state with  $2n$  extra Cooper pairs on one side of the Josephson junction. [See the discussion below Eq. (F4).] However, it has been derived quite differently here; in particular, we avoided any claim that the states  $|i, n\rangle$  have a simple physical interpretation in terms of the positions of Cooper pairs.

Assembling our results, we find the continuum limit of our matrix equation (F8):

$$\begin{aligned} & - \begin{bmatrix} E_{\odot;\odot} & E_{\odot;\odot} \\ E_{\odot;\odot} & E_{\odot;\odot} \end{bmatrix} \frac{d^2}{d\bar{\theta}^2} \begin{bmatrix} \psi(\odot, \bar{\theta}) \\ \psi(\odot, \bar{\theta}) \end{bmatrix} + \begin{bmatrix} (E_{\odot} - E_J \cos \frac{1}{2}(\bar{\theta} - \theta^{\odot}) + \frac{1}{2}E_L(\bar{\theta} - \theta^{\odot})^2) \psi(\odot, \bar{\theta}) \\ (E_{\odot} - E_J \cos \frac{1}{2}(\bar{\theta} - \theta^{\odot}) + \frac{1}{2}E_L(\bar{\theta} - \theta^{\odot})^2) \psi(\odot, \bar{\theta}) \end{bmatrix} \\ & = E \begin{bmatrix} \psi(\odot, \bar{\theta}) \\ \psi(\odot, \bar{\theta}) \end{bmatrix}. \end{aligned} \quad (\text{F12})$$

An approximate one-component equation can be obtained by adopting the ansatz

$$\begin{bmatrix} \psi(\odot, \bar{\theta}) \\ \psi(\odot, \bar{\theta}) \end{bmatrix} \approx \begin{cases} \begin{bmatrix} \psi(\bar{\theta}) \\ 0 \end{bmatrix}, & \bar{\theta} \leq \bar{\theta}_m \\ \begin{bmatrix} 0 \\ \psi(\bar{\theta}) \end{bmatrix}, & \bar{\theta} > \bar{\theta}_m \end{cases} = \begin{bmatrix} 1 - f(\bar{\theta}) \\ f(\bar{\theta}) \end{bmatrix} \psi(\bar{\theta}). \quad (\text{F13})$$

Here  $f(\bar{\theta})$  is a step function that increases from 0 to 1 when  $\bar{\theta}$  transitions through the local maximum  $\bar{\theta}_m$  defined by  $E_{\odot} - E_J \cos \frac{1}{2}(\bar{\theta}_m - \theta^{\odot}) + \frac{1}{2}E_L(\bar{\theta}_m - \theta^{\odot})^2 = E_{\odot} - E_J \cos \frac{1}{2}(\bar{\theta}_m - \theta^{\odot}) + \frac{1}{2}E_L(\bar{\theta}_m - \theta^{\odot})^2$ . When the rf-SQUID qubit is threaded by a half superconducting flux quantum, the symmetric double-well potential depicted in Fig. 2(d) has a local maximum at  $\bar{\theta}_m = 0$ . Inserting the ansatz, we are left with

$$-4E_C(\bar{\theta}) \frac{d^2}{d\bar{\theta}^2} \psi(\bar{\theta}) + E_I(\bar{\theta}) \psi(\bar{\theta}) = E \psi(\bar{\theta}), \quad (\text{F14})$$

where

$$4E_C(\bar{\theta}) = \begin{cases} E_{\odot;\odot}, & \bar{\theta} \leq \bar{\theta}_m, \\ E_{\odot;\odot}, & \bar{\theta} > \bar{\theta}_m, \end{cases}$$

and

$$E_I(\bar{\theta}) = \begin{cases} E_{\odot} - E_J \cos \frac{1}{2}(\bar{\theta} - \bar{\theta}^{\odot}) + \frac{1}{2}E_L(\bar{\theta} - \bar{\theta}^{\odot})^2, & \bar{\theta} \leq \bar{\theta}_m, \\ E_{\odot} - E_J \cos \frac{1}{2}(\bar{\theta} - \bar{\theta}^{\odot}) + \frac{1}{2}E_L(\bar{\theta} - \bar{\theta}^{\odot})^2, & \bar{\theta} > \bar{\theta}_m. \end{cases}$$

In this derivation, we neglect the off-diagonal values  $E_{\circ,\circ}$  and  $E_{\circ,\circ}$ , assuming that they are small compared to  $E_I(\bar{\theta})$ . We also neglect terms proportional to  $(df(\bar{\theta})/d\bar{\theta})(d\psi(\bar{\theta})/d\bar{\theta})$  or  $(d^2f(\bar{\theta})/d\bar{\theta}^2)\psi(\bar{\theta})$ . This is justified if  $\psi(\bar{\theta})$  and  $d\psi(\bar{\theta})/d\bar{\theta}$  are small at the local maximum  $\bar{\theta}_m$ , the only point at which  $df(\bar{\theta})/d\bar{\theta}$  and  $d^2f(\bar{\theta})/d\bar{\theta}^2$  do not vanish. For instance, this approximation seems particularly appropriate for low-energy eigenstates of a double-well potential that nearly vanish inside the potential barrier [see Fig. 2(d)].

### APPENDIX G: NUMBER OF ENTANGLED ELECTRONS

Computing the number of entangled electrons in an rf-SQUID qubit is beyond the scope of LE theory. One might attempt an answer within LE theory (see, e.g., Ref. [40]) by working in the basis  $|n\rangle$  and regarding  $n$  as the number of Cooper pairs on the capacitors shunting the Josephson junction of the qubit. For example, one might associate the uncertainty  $\Delta n$  with the number of Cooper pairs participating in the supercurrent by flowing on and off the junction capacitance. However, this association leads to unphysical conclusions. For the parameters of the rf-SQUID qubit experiment [25], for example, one computes  $\Delta n \sim 50$  pairs in the entangled state. Traveling with speed  $v$  around a ring of circumference  $L_z$ , they should produce a current  $I$  satisfying  $\Delta n \sim IL_z/2ev$ . Inserting  $L_z \sim 500 \mu\text{m}$  and  $I \sim \mu\text{A}$ , we find agreement only if  $v$  approaches the speed of light  $c$ . But physically, the maximum plausible speed is the Fermi velocity  $v_F \sim 0.01c$ .

Our theory provides a microscopic many-body quantum state of the rf-SQUID qubit, which is not provided by LE theory. We use this quantum state in the main text to evaluate Eq. (19). In this section, we give a short derivation of an approximate expression [27,28] for Eq. (19) that assumes that the many-body state is a superposition of displaced Fermi seas counterpropagating in a ring of circumference  $L_z$ . A displaced Fermi sea is a sphere of momentum eigenstates that is centered at a nonzero momentum. Thus, the basis that diagonalizes the expression  $\langle \circ | c_{\mathbf{Q}}^\dagger c_{\mathbf{Q}'} | \circ \rangle - \langle \circ | c_{\mathbf{Q}}^\dagger c_{\mathbf{Q}'} | \circ \rangle$  appearing in Eq. (19) is given by momentum and spin:  $\mathbf{Q} = (\mathbf{q}, \sigma)$ .

If the displaced Fermi seas carry current  $\pm I/2$  and are centered at momentum  $\pm q$  then the total number of electrons below the Fermi surface of each sea is  $N \sim IL_z/2e(q/m)$ , where  $m$  is the electron mass. However, not all  $N$  electrons are entangled when we superpose displaced Fermi seas. The core electronic states are occupied in both displaced Fermi seas; these core electronic states do not participate in the entanglement [27,28], and the sum (19) is deliberately defined so that they do not contribute. In Fig. 6(a), which depicts the two displaced Fermi seas graphically, these core electrons occupy the white region. Only the four colored slivers in Fig. 6(a) make contributions to

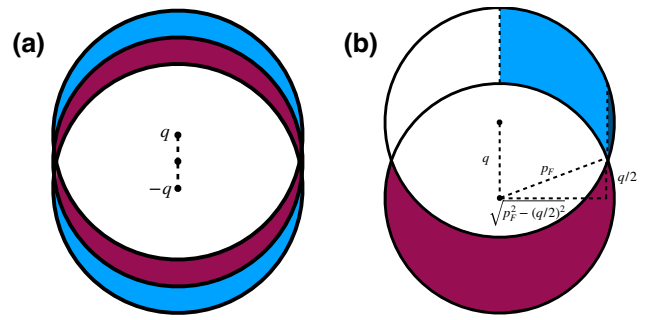


FIG. 6. (a) Cross section of three displaced Fermi seas, one shifted up by  $q$ , one shifted down by  $-q$ , and one undisplaced. If the blue slivers are exchanged and the purple approximate slivers are exchanged, the displaced Fermi seas are mapped into one other. Thus, the number of entangled electrons is the number of electronic states occupying one blue sliver and one purple sliver. (b) Diagram used to evaluate the volume of the sliver in momentum space. Upper circle, centered at  $q$ , and middle circle, centered at  $0$ , from (a) are depicted. Sliver is decomposed into several regions [the first term in Eq. (G1) proceeds over the light blue part and the second term in Eq. (G1) over the dark blue part].

Eq. (19). And, recalling the factor of  $1/2$  in Eq. (19), the quantity  $\Delta N$  equals the number of electronic states in one blue sliver plus one purple sliver. The slivers are approximately congruent, and we evaluate the volume of a blue sliver with the assistance of Fig. 6(b). If  $p_F$  is the Fermi momentum, the volume of the blue sliver in momentum space is

$$\begin{aligned} \int_{\text{Sliver}} d^3p &= \left[ 2\pi \int_0^{\sqrt{p_F^2 - (q/2)^2}} dp_r p_r \int_{\sqrt{p_F^2 - p_r^2}}^{q + \sqrt{p_F^2 - p_r^2}} dp_z \right. \\ &\quad \left. + 2\pi \int_{\sqrt{p_F^2 - (q/2)^2}}^{p_F} dp_r p_r \int_{q - \sqrt{p_F^2 - p_r^2}}^{q + \sqrt{p_F^2 - p_r^2}} dp_z \right] \\ &= \pi p_F^2 q - \frac{\pi}{24} q^3 \approx \pi p_F^2 q. \end{aligned} \quad (\text{G1})$$

We have performed the integral using cylindrical coordinates. In the final line, we assume that  $p_F \gg q$ . Intuitively, the light blue region of Fig. 6(b), rotated around the  $z$  axis, has approximately the volume of a cylinder of base  $\pi p_F^2$  and height  $q$ . The number of electronic states in one blue sliver plus one purple sliver in Fig. 6(a) is  $\Delta N \approx N(2\pi p_F^2 q)/(4\pi p_F^3/3) = N3q/2p_F$ , using the fact that the Fermi sea has volume  $4\pi p_F^3/3$  in momentum space. Substituting in the expression for  $N$  above, we find that  $\Delta N \sim 3IL_z/4e(p_F/m) = 3IL_z/4ev_F$ .

[1] P. Krantz, M. Kjaergaard, F. Yan, T. P. Orlando, S. Gustavsson, and W. D. Oliver, A quantum engineer's guide to superconducting qubits, *Applied Physics Reviews* 6, 021318 (2019).

- [2] Y. Nakamura, Y. A. Pashkin, and J. S. Tsai, Coherent control of macroscopic quantum states in a single-Cooper-pair box, *Nature* **398**, 786 (1999).
- [3] J. Mooij, T. Orlando, L. Levitov, L. Tian, C. H. V. der Wal, and S. Lloyd, Josephson persistent-current qubit, *Science* **285**, 1036 (1999).
- [4] J. M. Martinis, S. Nam, J. Aumentado, and C. Urbina, Rabi oscillations in a large Josephson-junction qubit, *Phys. Rev. Lett.* **89**, 117901 (2002).
- [5] D. Vion, A. Aassime, A. Cottet, P. Joyez, H. Pothier, C. Urbina, D. Esteve, and M. H. Devoret, Manipulating the quantum state of an electrical circuit, *Science* **296**, 886 (2002).
- [6] J. Koch, T. M. Yu, J. Gambetta, A. A. Houck, D. I. Schuster, J. Majer, A. Blais, M. H. Devoret, S. M. Girvin, and R. J. Schoelkopf, Charge-insensitive qubit design derived from the Cooper pair box, *Phys. Rev. A* **76**, 042319 (2007).
- [7] V. E. Manucharyan, J. Koch, L. I. Glazman, and M. H. Devoret, Fluxonium: Single Cooper-pair circuit free of charge offsets, *Science* **326**, 113 (2009).
- [8] F. Yan, S. Gustavsson, A. Kamal, J. Birenbaum, A. P. Sears, D. Hover, T. J. Gudmundsen, D. Rosenberg, G. Samach, S. Weber, T. L. Yoder, T. P. Orlando, J. Clarke, A. J. Kerman, and W. D. Oliver, The flux qubit revisited to enhance coherence and reproducibility, *Nat. Comm.* **7**, 12964 (2016).
- [9] M. H. Devoret and R. J. Schoelkopf, Superconducting circuits for quantum information: An outlook, *Science* **339**, 1169 (2013).
- [10] A. Somoroff, Q. Ficheux, R. A. Mencia, H. Xiong, R. Kuzmin, and V. E. Manucharyan, Millisecond coherence in a superconducting qubit, *Phys. Rev. Lett.* **130**, 267001 (2023).
- [11] M. H. Devoret, in *Les Houches Session LXIII* (Oxford University Press, Oxford, 1997).
- [12] S. M. Girvin, in *Quantum Machines: Measurement and Control of Engineered Quantum Systems*, edited by M. Devoret, R. Schoelkopf, B. Huard, and L. F. Cugliandolo (Oxford University Press, Oxford, 2014), p. 113.
- [13] L. I. Glazman and G. Catelani, Bogoliubov quasiparticles in superconducting qubits, *SciPost Phys. Lect. Notes* **31** (2021).
- [14] R. Barends, *et al.*, Superconducting quantum circuits at the surface code threshold for fault tolerance, *Nature* **508**, 500 (2014).
- [15] Y. Chen, *et al.*, Qubit architecture with high coherence and fast tunable coupling, *Phys. Rev. Lett.* **113**, 220502 (2014).
- [16] H. Paik, A. Mezzacapo, M. Sandberg, D. McClure, B. Abdo, A. Córcoles, O. Dial, D. Bogorin, B. Plourde, M. Steffen, A. Cross, J. Gambetta, and J. M. Chow, Experimental demonstration of a resonator-induced phase gate in a multiqubit circuit-QED system, *Phys. Rev. Lett.* **117**, 250502 (2016).
- [17] S. Sheldon, E. Magesan, J. M. Chow, and J. M. Gambetta, Procedure for systematically tuning up cross-talk in the cross-resonance gate, *Phys. Rev. A* **93**, 060302(R) (2016).
- [18] N. Ofek, A. Petrenko, R. Heeres, P. Reinhold, Z. Leghtas, B. Vlastakis, Y. Liu, L. Frunzio, S. M. Girvin, L. Jiang, M. Mirrahimi, M. H. Devoret, and R. J. Schoelkopf, Extending the lifetime of a quantum bit with error correction in superconducting circuits, *Nature* **536**, 441 (2016).
- [19] D. C. McKay, S. Filipp, A. Mezzacapo, E. Magesan, J. M. Chow, and J. M. Gambetta, Universal gate for fixed-frequency qubits via a tunable bus, *Phys. Rev. Applied* **6**, 064007 (2016).
- [20] M. Kjaergaard, *et al.*, Programming a quantum computer with quantum instructions, *ArXiv:2001.08838* (2020).
- [21] S. S. Hong, A. T. Papageorge, P. Sivarajah, G. Crossman, N. Didier, A. M. Polloreno, E. A. Sete, S. W. Turkowski, M. P. da Silva, and B. R. Johnson, Demonstration of a parametrically activated entangling gate protected from flux noise, *Phys. Rev. A* **101**, 012302 (2020).
- [22] H. Zhang, S. Chakram, T. Roy, N. Earnest, Y. Lu, Z. Huang, D. K. Weiss, J. Koch, and D. I. Schuster, Universal fast-flux control of a coherent, low-frequency qubit, *Phys. Rev. X* **11**, 011010 (2021).
- [23] R. Acharya, *et al.*, Suppressing quantum errors by scaling a surface code logical qubit, *ArXiv:2207.06431* (2022).
- [24] D. A. Ivanov and M. V. Feigel'man, Two-level Hamiltonian of a superconducting quantum point contact, *Phys. Rev. B* **59**, 8444 (1999).
- [25] J. R. Friedman, V. Patel, W. Chen, S. K. Tolpygo, and J. E. Lukens, Quantum superposition of distinct macroscopic states, *Nature* **406**, 43 (2000).
- [26] C. H. Van der Wal, A. C. J. ter Haar, F. K. Wilhelm, R. N. Schouten, C. J. P. M. Harmans, T. P. Orlando, S. Lloyd, and J. E. Mooij, Quantum superposition of macroscopic persistent-current states, *Science* **290**, 773 (2000).
- [27] J. I. Korsbakken, F. K. Wilhelm, and K. B. Whaley, Electronic structure of superposition states in flux qubits, *Phys. Scr.* **T137**, 014022 (2009).
- [28] J. I. Korsbakken, F. K. Wilhelm, and K. B. Whaley, The size of macroscopic superposition states in flux qubits, *Euro. Phys. Lett.* **89**, 30003 (2010).
- [29] P. G. de Gennes, *Superconductivity of Metals and Alloys* (W. A. Benjamin, Inc., New York, 1966).
- [30] V. Ambegaokar, U. Eckern, and G. Schon, Quantum dynamics of tunneling between superconductors, *Phys. Rev. Lett.* **48**, 1745 (1982).
- [31] J.-X. Zhu, *Bogoliubov-De Gennes Method and Its Applications* (Springer, 2016).
- [32] N. Onishi and S. Yoshida, Generator coordinate method applied to nuclei in the transition region, *Nucl. Phys.* **80**, 367 (1966).
- [33] P. Ring and P. Schuck, *The Nuclear Many-Body Problem* (Springer, New York, 2004), p. 615.
- [34] J. A. Schreier, A. A. Houck, J. Koch, D. I. Schuster, B. R. Johnson, J. M. Chow, J. M. Gambetta, J. Majer, L. Frunzio, M. H. Devoret, S. M. Girvin, and R. J. Schoelkopf, Suppressing charge noise decoherence in superconducting charge qubits, *Phys. Rev. B* **77**, 180502 (2008).
- [35] C. Wang, C. Axline, Y. Y. Gao, T. Brecht, Y. Chu, L. Frunzio, M. H. Devoret, and R. J. Schoelkopf, Surface participation and dielectric loss in superconducting qubits, *Appl. Phys. Lett.* **107**, 162601 (2015).
- [36] H. Mamin, B. Trimm, E. Huang, S. Carnevale, C. Retner, N. Arellano, M. Sherwood, C. Kurter, M. Sandberg, R. Shelby, M. Mueed, B. Madon, A. Pushp, M. Steffen, and D. Rugar, Merged-element transmons: Design and qubit performance, *Phys. Rev. Applied* **16**, 024023 (2021).

- [37] J.-X. Zhu and Z. D. Wang, Supercurrent determined from the Aharonov-Bohm effect in mesoscopic superconducting rings, *Phys. Rev. B* **50**, 7207 (1994).
- [38] A. J. Leggett and A. Garg, Quantum mechanics versus macroscopic realism: Is the flux there when nobody looks? *Phys. Rev. Lett.* **54**, 857 (1985).
- [39] F. Frowis, P. Sekatski, W. Dur, N. Gisin, and N. Sangouard, Macroscopic quantum states: Measures, fragility, and implementations, *Rev. Mod. Phys.* **90**, 025004 (2018).
- [40] F. Marquardt, B. Abel, and J. von Delft, Measuring the size of a quantum superposition of many-body states, *Phys. Rev. A* **78**, 012109 (2008).